

University of Alberta

DESIGN OF OPTIMAL FRAMEWORKS FOR WIDEBAND/MULTICHANNEL
SPECTRUM SENSING IN COGNITIVE RADIO NETWORKS

by

Pedram Paysarvi Hoseini

A thesis submitted to the Faculty of Graduate Studies and Research
in partial fulfillment of the requirements for the degree of

Master of Science
in
Communication

Department of Electrical and Computer Engineering

© Pedram Paysarvi Hoseini

Spring 2011

Edmonton, Alberta

Permission is hereby granted to the University of Alberta Libraries to reproduce single copies of this thesis and to lend or sell such copies for private, scholarly or scientific research purposes only. Where the thesis is converted to, or otherwise made available in digital form, the University of Alberta will advise potential users of the thesis of these terms.

The author reserves all other publication and other rights in association with the copyright in the thesis, and except as herein before provided, neither the thesis nor any substantial portion thereof may be printed or otherwise reproduced in any material form whatever without the author's prior written permission.

Examining Committee

Norman C. Beaulieu, Electrical and Computer Engineering

Ioanis Nikolaidis, Computing Science

Ashwin K. Iyer, Electrical and Computer Engineering

To my lovely wife...

for her care, patience and unremitting love...

and to my beloved parents...

for their encouragement, support and advice

Abstract

Several optimal detection frameworks for wideband/multichannel spectrum sensing in cognitive radio networks are proposed. All frameworks search for multiple secondary transmission opportunities over a number of narrowband channels, enhancing the secondary network performance while respecting the primary network integrity and keeping the interference limited. Considering a periodic sensing scheme with either uniform or non-uniform channel sensing durations, the detection problems are formulated as joint optimization of the sensing duration(s) and individual detector parameters to maximize the aggregate achievable secondary throughput capacity given some bounds/limits on the overall interference imposed on the primary network. It is demonstrated that all the formulated optimization problems can be solved using “convex” optimization if certain practical constraints are applied. Simulation results attest that the proposed frameworks achieve superior performance compared to contemporary frameworks. To realize efficient implementation, an iterative low-complexity algorithm which solves one of the optimization problems with much lower complexity compared to other numerical methods is presented. It is established that the iteration-complexity and the complexity-per-iteration of the proposed algorithm increases linearly with the number of optimization variables (i.e. the number of narrowband channels).

Acknowledgements

First and foremost, I would like to express my deepest gratitude to my supervisor, Prof. Norman C. Beaulieu, who has truly helped me throughout my research and has always supported me in any possible way. Without his vast knowledge, tactful experience and great supervision, this project would not have been successful.

I also wish to sincerely thank Dr. Ioanis Nikolaidis and Dr. Ashwin K. Iyer for their willingness to serve as my examining committee members, for reviewing my thesis and specially for their valuable comments and feedback.

My keen appreciations goes to Dr. AmirMasoud Rabiei and Dr. Reza Nikjah who, as my good friends and as senior members of *i*CORE Wireless Communications Laboratory (*i*WCL), helped me a lot during the course of my graduate study. I would also like to thank my dear friend, Ramin Babaei, who has always been supportive and helpful during all the years of our friendship.

I am extremely grateful to my other lab-mates in *i*WCL for creating a professional and vibrant environment which enabled me to enrich my graduate experience. I would also like to extend my appreciation to my other Edmontonian and non-Edmontonian friends for their guidance and help in both academic and non-academic endeavors.

Last but not least, My heartfelt thanks is dedicated to my dear parents and my lovely wife, Nastaran, for their tremendous support, care, encouragement and love.

Table of Contents

1	Introduction	1
1.1	Cognitive Radio	1
1.2	Spectrum Sensing	3
1.3	Motivations	4
1.4	Related Works and Challenges	4
1.5	Contributions	5
1.6	Thesis Outline	7
2	Background and System Model	8
2.1	Background	8
2.1.1	Signal Detection for Spectrum Sensing	8
2.1.2	Energy Detection	9
2.2	System Model	11
2.2.1	Wideband Channel	11
2.2.2	Periodic Sensing	12
2.3	Summary	13
3	Wideband Spectrum Sensing With Uniform Channel Sensing Durations	14
3.1	Primary Communication	14
3.1.1	Received Primary Signals	15
3.1.2	Signal Detection in Each Subchannel	16
3.2	Optimal Multiband Sensing-Time-Adaptive Joint Detection Framework	18

3.2.1	Problem Formulation	19
3.2.2	Minimum Value of Sensing Time τ	21
3.2.3	Convex Optimization	21
3.2.4	Large-Period Regimes	23
3.2.5	Multiband Joint Detection Framework	25
3.3	Efficient Implementation of the Multiband Sensing-Time-Adaptive Joint Detection Framework	26
3.3.1	Constant τ	27
3.3.2	Dual Problem	28
3.3.3	Efficient Algorithm for the Multiband Joint Detection	30
3.3.4	Efficient Algorithm for Multiband Sensing-Time-Adaptive Joint Detection	34
3.4	Simulation Results	37
3.4.1	Example 1: Multiband Sensing-Time-Adaptive Joint Detection Framework	38
3.4.2	Example 2: Efficient Low-Complexity Wideband Sensing Algorithm	41
3.5	Summary	43
4	Multichannel Spectrum Sensing With Non-Uniform Channel Sensing Durations	46
4.1	System Model	46
4.1.1	Sequential Periodic Sensing	47
4.1.2	Signal Detection in Each Channel	48
4.2	Optimal Multichannel Spectrum Sensing Framework - Generic Perspective	49
4.2.1	Problem Formulation	50
4.2.2	Minimum Value of Sensing Time τ	51
4.2.3	Convex Optimization	51
4.2.3.1	Uniform Sensing Subslots	52
4.2.3.2	Non-Uniform Sensing Subslots	53
4.2.4	Large-Period Regimes	55

4.3	Optimal Multichannel Spectrum Sensing Framework - Decoupled Perspective	56
4.3.1	Detection Problem	56
4.3.2	Convex Optimization	58
4.3.2.1	Uniform Sensing Subslots	58
4.3.2.2	Non-Uniform Sensing Subslots	59
4.4	Simulation Results	62
4.4.1	Example 1: Sequential Multichannel Joint Detection Framework	62
4.4.2	Example 2: Decoupled Sequential Multichannel Joint Detection Framework	64
4.5	Summary	66
5	Conclusion and Future Research Directions	68
5.1	Conclusion	68
5.2	Future Research Directions	70
	References	71

List of Tables

3.1	Typical system parameter set used for the simulation - wideband sensing with uniform channel sensing durations	38
4.1	Typical system parameter set used for the simulation - multichannel sensing with non-uniform channel sensing durations	63

List of Figures

2.1	Probabilities of false alarm and missed detection vs. detection threshold, for signal-to-noise ratio, $\gamma = 0.8$ and noise power density, $\sigma_w^2 = 1$	11
2.2	An illustrative example of a wideband/multichannel scenario and the subchannel occupancies.	12
2.3	The frame structure of periodic spectrum sensing.	13
3.1	The multiband sensing-time-adaptive joint detection framework for wideband spectrum sensing.	18
3.2	An example of the maximum and minimum values associated with $\bar{\lambda}_1$ in each subchannel k and their mappings to the $\bar{\lambda}_1 > 0$ axis. . . .	34
3.3	The available opportunistic throughput for cognitive radio transmission vs. the aggregate interference to the primary network.	39
3.4	The number of samples vs. the SNR increment (dB) above the SNRs, γ_k , listed in Table 3.1, when the aggregate interference to the primary network $\xi = 1$ and $f_s T = 8000$	40
3.5	The available opportunistic throughput for cognitive transmission vs. the normalized minimum sensing time $\tau_{\min}^{\text{norm}}$, when the aggregate interference to the primary network $\xi = 1$	40
3.6	The available opportunistic throughput for cognitive radio transmission vs. the aggregate interference to the primary network.	41

3.7	The average running time used for implementation of the MJD framework vs. the number of narrowband subchannels in the wideband spectrum, when the aggregate interference to the primary user $\xi = 1$ and $\ c\ = 15$	42
3.8	The available opportunistic throughput for cognitive radio transmission vs. the initial number of samples defined in Algorithm 3.2, when the aggregate interference to the primary user $\xi = 1$	43
3.9	The probability of missed detection obtained in each iteration of Algorithm 3.2, when the aggregate interference to the primary user $\xi = 1$	44
4.1	The frame structure of the sequential periodic sensing.	47
4.2	The sequential multiband joint detection framework for multichannel spectrum sensing.	49
4.3	The available opportunistic throughput for cognitive radio transmission vs. the aggregate interference to the primary network.	64
4.4	The number of samples vs. the SNR increment (dB) above the SNRs, γ_k , listed in Table 4.1, when the aggregate interference to the primary network $\xi = 1$	65
4.5	The available opportunistic throughput for cognitive transmission vs. the normalized minimum sensing time $\tau_{\min}^{\text{norm}}$, when the aggregate interference to the primary network $\xi = 1$	65
4.6	The available opportunistic throughput vs. the SNR increment (dB) above the SNRs, γ_k , listed in Table 4.1.	66

List of Algorithms

3.1	Low-Complexity Implementation of the MJD Framework	35
3.2	Low-Complexity Implementation of the proposed MSJD Framework	37

List of Symbols

M	Number of samples used for sensing the wideband spectrum	13
M_k	Number of samples used for sensing channel k	47
N	Number of narrowband channels in wideband spectrum	11
T	Frame duration in the periodic sensing scheme	12
T_k	Decision statistics of the k -th channel	16
α_k	Maximum allowable probability of interference in channel k	20
α'_k	Maximum allowable interference detection for D-SMJD framework	57
β_k	Minimum transmission opportunity detection expected in channel k	20
γ_k	Received signal-to-noise ratio of the k -th channel	17
λ_1	Lagrangian dual variable associated with (C3.5)	28
$\lambda_{2(3)}^{(k)}$	Lagrangian dual variable associated with (C3.6)	28
$\mathcal{H}_{0,k}$	Hypothesis of primary user's absence in the k -th channel	12
$\mathcal{H}_{1,k}$	Hypothesis of primary user's presence in the k -th channel	12
σ_w^2	Noise power density	15
τ	Sensing time slot	13
τ_k	Sensing time subslot used for sensing the k -th channel	47
τ_{\max}	Maximum allowable sensing time	20

τ_{\min}	Minimum Value of Sensing Time τ	21
$\tau_{\min}^{\text{norm}}$	Normalized minimum sensing time	24
ε_k	Decision threshold in the k -th channel	17
$\varepsilon_{k,\max}$	Maximum allowable detection threshold in the k -th channel for the MJD framework	27
$\varepsilon_{k,\min}$	Minimum allowable detection threshold in the k -th channel for the MJD framework	27
ξ	Maximum aggregate interference tolerated by the primary network	20
c_k	Cost of interfering primary user in the k -th channel	19
f_s	Sensing sampling frequency	13
r_k	Opportunistic throughput of secondary user at channel k when operating in the absence of primary users	19

List of Abbreviations

AWGN	additive white Gaussian noise	8
CDF	cumulative distribution function	9
CR	cognitive radio	1
D-SMJD	decoupled sequential multichannel joint detection	7
DFT	discrete Fourier transform	15
DSA	dynamic spectrum access	1
FCC	Federal Communications Commission	1
KKT	Karush-Kuhn-Tucker	28
MJD	multiband joint detection	5
MSJD	multiband sensing-time-adaptive joint detection	5
OFDM	orthogonal frequency division multiplexing	4
PSK	phase-shift-keying	9
SMJD	sequential multichannel joint detection	6
SNR	signal-to-noise ratio	3
WRAN	Wireless Regional Area Network	2

Chapter 1

Introduction

The ability to access and utilize the electromagnetic radio spectrum as a communication medium gave birth to wireless communications technology which has attracted a great deal of telecommunication researchers during the recent years. In order to avoid interference between different wireless applications, and to facilitate its utilization management, the wireless radio spectrum has been divided into multiple portions. Each portion has been assigned to a specific license holder (primary user) on a long-term basis. Over time, due to the ever-growing need for wireless communications and lack of remaining unlicensed frequency resources, this fixed spectrum assignment policy has led to the *spectrum scarcity* problem.

1.1 Cognitive Radio

The so-called spectrum scarcity problem is mainly due to significant over-allocation and under-utilization of the wireless spectrum rather than due to physical shortage of the spectrum. Recent measurements, performed by the U.S. Federal Communications Commission (FCC) [1], have witnessed that depending on time and geographical location, most of the licensed frequency bands are being exploited sporadically (i.e. not efficiently) and are available for other possible applications. Therefore, in order to realize efficient spectrum utilization, the static spectrum access must be replaced by dynamic spectrum access (DSA) [2].

The key technology behind the dynamic spectrum access is cognitive radio (CR), which has recently been proposed to revolutionize the wireless communication sys-

tems [3]. The aim of CR is to enhance the overall spectrum utilization efficiency by allowing the unlicensed (secondary) users to opportunistically access the vacant frequency bands (i.e. spectrum holes) without compromising the primary network's integrity and imposing unwanted and harmful interference on it [4]. It presents an intelligent and highly reliable wireless communication system with the ability of exploiting the spectrum in an optimal manner by interacting with its surrounding, learning from the environment and adjusting its parameters to improve the overall communication quality-of-service [5]. It has been recognized as an excellent candidate for the next generation wireless networks and has already been adopted in emerging wireless access standards such as IEEE 802.22- Wireless Regional Area Networks (WRANs) [6].

A CR network is designed to be aware of its surroundings and is allowed to access only the unused portion of the spectrum. In order for CR systems to fulfill this task, different crucial functionalities must be accomplished, which are as follows:

1- *Spectrum Sensing* carries out the essential task of monitoring the primary user activities and sensing the radio spectrum in order to reliably locate suitable opportunities for transmission.

2- *Spectrum Management* is employed to manage the process of selecting the best available channel among all vacant spectrum which meets the secondary user communication requirements and quality of service requirements, and maximizes the spectrum efficiency.

3- *Spectrum Mobility* serves the task of vacating the spectrum when the legacy (primary) user re-appears and decides to re-utilize the spectrum. It also has to switch to a better channel when the current channel becomes unavailable or doesn't meet the user specifications. It is designed to maintain seamless secondary communications during the transition to the better channel.

4- *Spectrum Sharing* is to control fair distribution of the available frequency bands to a potentially large number of secondary users and to coordinate their access.

1.2 Spectrum Sensing

Spectrum sensing, as a crucial functionality in CR networks, accomplishes the key task of locating vacant bandwidth portions (i.e. opportunities for CR transmission), without harmfully interfering with the primary network communication [5]. The challenge for a reliable sensing method is when the primary received signal is very weak or deeply faded/shadowed (i.e. low signal-to-noise ratio (SNR) regimes) [7].

Several spectrum sensing techniques have been proposed so far which can be categorized into three general groups, energy detection [8], coherent detection [9] and cyclostationary feature detection [10]. The energy detection strategy simply computes the energy of the received signal as a decision statistic and compares it to a threshold. This technique is known to be optimal when the only information available about the primary received signal is the noise power density and the received primary signal samples are independent and identically distributed [11]. In the case of correlated samples, an eigenvalue-based method which exploits the ratio of the maximum and minimum eigenvalues of the covariance matrix can be used [12].

If some knowledge of other features of the primary signal such as the modulation scheme, pilot information, synchronization symbols, etc. are available at the cognitive radio receiver, a coherent detector or cyclostationary feature detector may be exploited in order to have more robust sensing [13]. On the one hand, coherent detection, also known as matched filter detection, can enhance the detection performance when the primary transmitted signal is deterministic and known to the secondary network [14]. On the other hand, since most of the primary signals are modeled as sinusoidal carriers, some periodicity pattern can be extracted from the received signals [15]. Thus, cyclostationary feature detection, which uses the inherent built-in-periodicity of the received signal, can be exploited for more accurate detection. However, due to its low computational (and hence implementation) complexities and its fast detection ability, energy detection is widely deployed as the underlying detection scheme and is exploited as the building block in this thesis, as well. Meanwhile, various cooperation methods between multiple secondary nodes has been developed to enhance the detection agility (see [16] and the references therein). A survey on spectrum sensing algorithms can be found in [17], [18].

1.3 Motivations

In most of the previous works, the studies on spectrum sensing are limited to sensing single narrowband channels. There are rather limited prior works, when it comes to wideband spectrum sensing. However, due to its cruciality and importance in CR networks, the number of works in this area is dramatically increasing.

Sensing multiple narrowband channels (or a wideband spectrum) represents an important, yet challenging topic in CR systems. In fact, it is recognized as one of the main requirements of an effective and practical CR system. Having a wideband (i.e. multichannel) sensing capability at the secondary RF front-end results in identifying multiple transmission opportunities which enables the CR coordinator to choose the “best available channel” [4]. It also enables improved sensing decision and improved design of other essential functionalities such as spectrum mobility and spectrum management [4].

1.4 Related Works and Challenges

An early approach was to have a tunable narrowband bandpass filter to sense a number of channels, one at a time [19]. There also have been some works on sensing multiple channels simultaneously. In [20], [21], the authors have used a wavelet approach to estimate the power spectral density (PSD) of the received primary signal and decompose it into a number of non-overlapping subbands. Likewise, the authors in [22], proposed an invariant generalized likelihood ratio (GLR) detector under the assumption that a minimum number of subbands are vacant and the noise and primary signal variances are unknown to monitor.

There are also some studies on the application of compressive sensing in wideband sensing [23]–[27]. In [28], the authors have considered an orthogonal frequency division multiplexing (OFDM) based CR system and have proposed a two-stage wideband detector under the assumption that the primary user appears at a segment of continuous subcarriers. The authors in [29] have proposed a maximum likelihood (ML) reconstruction of the spectrum when the spectral shape of the primary transmission is assumed to be known *a priori* to the CR users. Other recent

works on wideband spectrum sensing can be found in [30]–[32]. However, none of these studies have considered sensing multiple channels *jointly*, which is essential for implementing a maximally effective secondary network. Consequently, through a different approach, a novel “multiband joint detection” (MJD) framework for wideband sensing was proposed in [33] where the decisions are *jointly* made over multiple frequency bands.

More specifically, in the MJD framework [33], a set of individual secondary detectors are optimized so as to enhance the cognitive radio performance while protecting the primary network from harmful interference. Although the MJD framework represents a remarkable advancement in wideband sensing, some basic potentials of the system model have not been exploited. For instance, it is indeed crucial to sense the channel periodically since the spectrum must be vacated when a primary user reappears [34]–[38], a feature missing from the MJD framework. In addition, due to the wireless channel fluctuations and fading effects, it is essential to dynamically balance the quality and speed of sensing through an adaptive selection of the sensing time, which is assumed to be fixed in MJD. Moreover, considering a unified framework in which the sensing time and individual detector parameters are jointly optimized is mandatory for designing a maximally effective cognitive radio network.

1.5 Contributions

The major contributions of this work are threefold. First, we present an optimal framework for wideband spectrum sensing with uniform channel sensing durations which is referred to as multiband sensing-time-adaptive joint detection (MSJD). Adding periodic sensing to the system model used in [33] and considering the aforementioned design concerns, we maximize the achievable opportunistic throughput of the secondary user while keeping the interference with the primary network bounded to a reasonably low level. More specifically, we formulate our problem as a joint optimization of the sensing slot duration and individual channel parameters, where the objective function is the throughput capacity of the secondary user and the constraint is the aggregate (weighted) interference to the primary users. Furthermore, we show that our problem, which is generally non-convex, can be solved as a convex

optimization problem if certain practical constraints are imposed.

In addition, we propose an efficient algorithm which quickly and effectively computes the optimal sensing parameters within the aforementioned MSJD framework. In particular, taking advantage of Lagrangian duality properties presented in [39], we transform the original optimization problem into a class of equivalent subproblems and solve them accordingly. It is also demonstrated that the computational (hence implementation) complexity of the proposed algorithm is much lower than that of other commonly used numerical approaches such as the interior-point methods. In particular, we demonstrate that the iteration-complexity and the complexity-per-iteration of the proposed algorithm increases linearly as the number of primary individual channels increases. This level of complexity is very interesting from a practical/implementation viewpoint since it is remarkably time- and cost-effective.

In the MSJD framework, the sensing time slot is assumed to be the same (i.e. uniform) for all the frequency bands, owing to the nature of the wideband primary signal. In the third study, we assume that adopting different sensing durations for individual narrowband channels is viable. Consequently, considering a sequential periodic sensing scheme, we propose two optimal multichannel spectrum sensing frameworks. Specifically, we assume that multiple primary narrowband channels are sensed sequentially using a periodic sensing approach. We also assume that the amount of time used for sensing different channels can be chosen non-uniformly. That is, the channels-under-sense can assume different sensing time durations. This feature is shown to greatly improve the sensing performance. Given this, we propose to maximize the opportunistic secondary network throughput capacity, while limiting the interference imposed on the primary users. Particularly, we formulate the multichannel sensing problem as a joint optimization of the overall sensing time slot, the sensing subslots (dedicated for sensing individual channels) and individual detector parameters. While the objective function is the secondary throughput, the constraint function(s) is/are the overall interference on the primary network.

The first framework, referred to as “sequential multichannel joint detection” (SMJD) considers the aggregate interference on the primary network as the constraint function. Specifically, within the SMJD framework some relative priority coefficients, which characterize the relative costs incurred if the primary commu-

nications in the corresponding channels are interfered with, are assigned to every individual channel. That is, the overall probability of interference is aggregated (weighted) into a single functional form. In the second framework, known as “decoupled sequential multichannel joint detection” (D-SMJD), we assume that such cost/priority coefficients used in the aggregate interference function are difficult to define for some specific applications, resulting in a tractable mathematical description of the aggregate interference being unattainable. Therefore, within the D-SMJD, we assume that the probability of interference on each channel is limited independently, making the individual channels partially decoupled. Both formulated optimization problems, which are shown to be non-convex, are transformed into convex optimization problems under certain practical conditions. The transformation makes it tractable and efficient to find the global optimum solutions. Generally speaking, all the proposed frameworks make efficient use of the spectrum by establishing a suitable tradeoff between the secondary user access and primary network protection through a joint adjustment of the sensing parameters.

1.6 Thesis Outline

This thesis is organized as follows. In Chapter 2, we first present some background on signal detection for spectrum sensing which leads to the basic system model. In Chapter 3, we introduce the multiband sensing-time-adaptive joint detection (MSJD) framework for wideband sensing, which is followed by the presentation of the efficient algorithm for implementation of the proposed MSJD framework. The sequential multichannel joint detection (SMJD) framework which assumes non-uniform channel sensing durations is given in Chapter 4. Finally, Chapter 5 concludes this thesis while giving some suggestions and potential future research directions.

Chapter 2

Background and System Model

In this chapter, we first explain some background on signal detection for spectrum sensing and then present the general system model used in this study.

2.1 Background

2.1.1 Signal Detection for Spectrum Sensing

Spectrum sensing functionality allows the secondary user to detect the spectral holes (i.e. spectrum vacancies) and to opportunistically access them without imposing harmful interference to the primary network. To do so, binary hypothesis testing is exploited to differentiate between the faded primary received signal corrupted by the noise signal and the noise signal only. The mathematical representation of the binary testing is as follows:

$$\begin{aligned}\mathcal{H}_0 & : r(m) = w(m), & m = 1, 2, \dots, M \\ \mathcal{H}_1 & : r(m) = s(m) + w(m), & m = 1, 2, \dots, M\end{aligned}\tag{2.1}$$

where \mathcal{H}_0 denotes the absence of the primary signal, i.e. the baseband received primary signal at the secondary user contains noise only which is often assumed to be additive white Gaussian noise (AWGN), $w(m) \sim \mathcal{CN}(0, \sigma_w^2)$, and \mathcal{H}_1 represents the presence of the primary signal $s(m)$ which has been corrupted by $w(m)$. In addition, M corresponds to the primary signal measurements (i.e. samples)

used for sensing. In order to make a robust decision, all the received samples $\mathbf{r} = [r(1), r(2), \dots, r(M)]$ must be combined into a single functional form known as the decision statistic.

2.1.2 Energy Detection

Noncoherent energy detection (or radiometry) [14] is known to be one of the simplest methods for binary hypothesis testing. It is also known to be optimal when the only information available about the primary received signal is the noise power density and the received primary signal samples are independent and identically distributed (i.i.d.) [11]. The energy detector decision statistic is given by

$$T(\mathbf{r}) = \frac{1}{M} \sum_{m=1}^M |r(m)|^2 \underset{\mathcal{H}_0}{\overset{\mathcal{H}_1}{\gtrless}} \varepsilon \quad (2.2)$$

where $T(\mathbf{r})$ is the decision statistic and ε denotes the decision threshold. Usually $T(\mathbf{r})$ has a chi-square distribution under both hypotheses [8]. However, in order to facilitate the analysis, a central limit theorem [40] is used to approximate the cumulative distribution function (CDF) of $T(\mathbf{r})$ as a normal distribution under both hypotheses, i.e.,

$$T(\mathbf{r}) \sim \begin{cases} \mathcal{N}(\mu_0, \sigma_0), & \text{under } \mathcal{H}_0 \\ \mathcal{N}(\mu_1, \sigma_1), & \text{under } \mathcal{H}_1 \end{cases} \quad (2.3)$$

where μ_i , $\{i = 0, 1\}$ denotes the mean of $T(\mathbf{r})$ under \mathcal{H}_i and σ_i , $\{i = 0, 1\}$ represents its variance. Considering the modulation of the primary signal as complex-valued phase-shift-keying (PSK), one has

$$\mu_0 = \sigma_w^2 \quad (2.4)$$

$$\mu_1 = (\gamma + 1)\sigma_w^2 \quad (2.5)$$

and

$$\sigma_0 = \sigma_w^4/M \quad (2.6)$$

$$\sigma_1 = (2\gamma + 1)\sigma_w^4/M \quad (2.7)$$

where

$$\gamma = \frac{p_s}{\sigma_w^2} \quad (2.8)$$

is the received signal-to-noise ratio (*SNR*) and $p_s = \|s(m)\|/M$ represents the average primary signal power. The empirical average power, p_s , is often replaced by the statistical average power, $\mathbb{E} [|s(m)|^2]$, for a large number of samples, M , where $\mathbb{E}[\cdot]$ denotes expectation. In the detection context, there are two key error functions which determine the overall detection performance, probability of false alarm and probability of missed detection. The probability of false alarm is defined as the probability of deciding \mathcal{H}_1 when \mathcal{H}_0 is true, and is given mathematically by

$$P_f = Pr(T(\mathbf{r}) > \varepsilon | \mathcal{H}_0) = Q\left(\frac{\varepsilon - \mu_0}{\sigma_0}\right) \quad (2.9)$$

and the probability of missed detection, which is the probability of deciding \mathcal{H}_0 when \mathcal{H}_1 is true, is given by

$$P_m = 1 - Pr(T(\mathbf{r}) > \varepsilon | \mathcal{H}_1) = 1 - Q\left(\frac{\varepsilon - \mu_1}{\sigma_1}\right) \quad (2.10)$$

where

$$Q(x) = \frac{1}{\sqrt{2\pi}} \int_x^{+\infty} e^{-y^2/2} dy \quad (2.11)$$

denotes the complementary distribution function of the standard Gaussian distribution [41]. We point out that these two probabilities are both a function of the decision threshold ε and the number of samples M . One would like to minimize both the probability functions, however this is not feasible due to the inherent tradeoff between them.

The threshold ε is a tradeoff factor between the probabilities of false alarm and missed detection; a low threshold value will result in high false alarm probability in favor of low missed detection probability and vice versa. Although increasing the number of samples, M , would decrease both error functions, we indicate that the choice of the number of samples M is also a tradeoff between the “quality” and “speed” of sensing. By increasing the number of samples (the sensing time), the test decision is more accurate but the available time for cognitive radio transmission is

reduced, in consequence (refer to Section 2.2.2). These concerns mandate designing an efficient sensing framework which wisely balances these parameters, specifically when sensing is performed over a wideband channel. In order to make our argument convincingly, Fig. 2.1 plots the probabilities of false alarm and missed detection versus the decision threshold for two different numbers of samples.

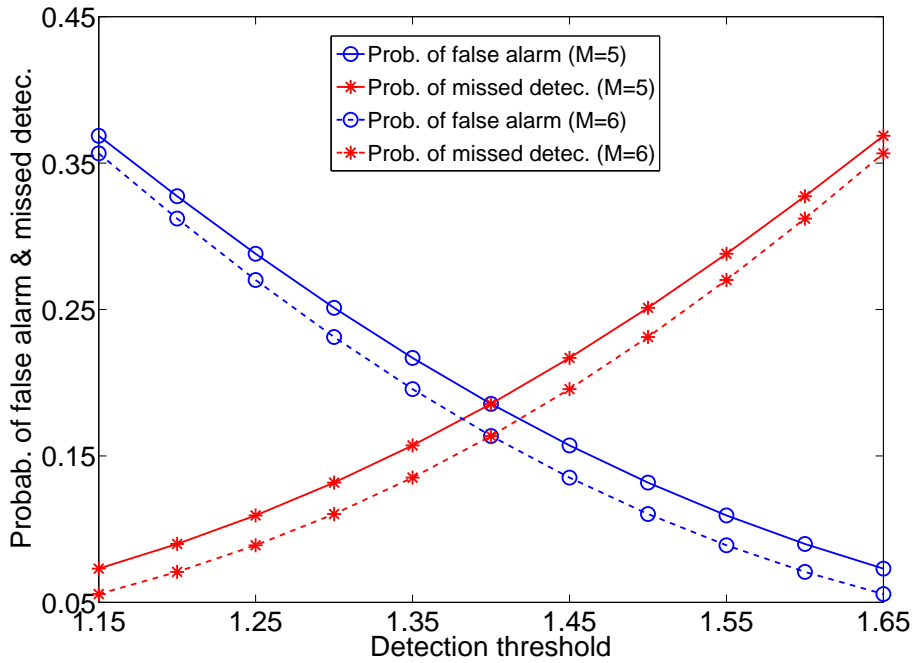


Fig. 2.1. Probabilities of false alarm and missed detection vs. detection threshold, for signal-to-noise ratio, $\gamma = 0.8$ and noise power density, $\sigma_w^2 = 1$.

2.2 System Model

2.2.1 Wideband Channel

We consider a primary communication network operating over a wideband spectrum, which is decomposed into N non-overlapping narrowband frequency bands (subchannels). Depending on time and geographical area, some of these subchannels might not be utilized by the primary users and are available for the cognitive radio transmission. Fig. 2.2 shows an illustrative example of such wideband channel. As shown in the figure, some of the subbands (labeled as "0") are not used and can be opportunistically accessed by the secondary users. The crucial task of

spectrum sensing is to reliably detect these vacant frequency bands while respecting the integrity of the primary network.

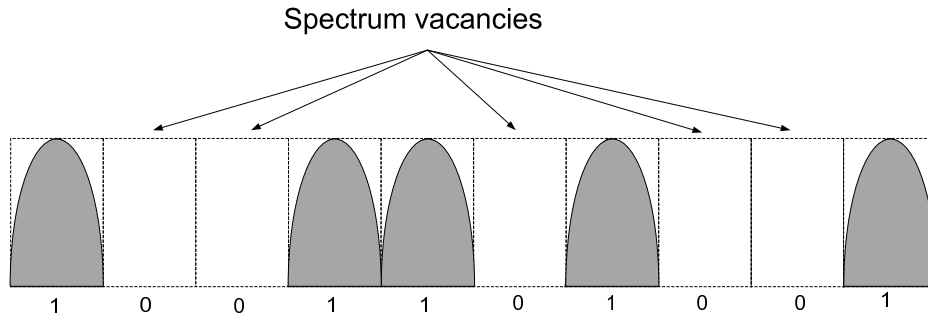


Fig. 2.2. An illustrative example of a wideband/multichannel scenario and the subchannel occupancies.

For modeling the detection problem on each subchannel k , binary hypothesis testing is used in which hypothesis $H_{0,k}$ represents the absence of the primary signal and hypothesis $H_{1,k}$ represents the presence of the primary signal. For simplicity, we assume that during the time that a cognitive radio performs sensing, other peers remain passive such that the only signal in the whole bandwidth is the one transmitted by the primary users. This can be assured by the higher-layer protocols. In this study, instead of sensing each channel independently, we develop a sensing scheme which jointly detects the opportunities for secondary transmission over the entire target spectral bandwidth. That is, instead of sensing one channel at a time, we consider a joint detection framework which detects channel vacancies over the whole spectrum.

2.2.2 Periodic Sensing

Once a secondary user detects an opportunity for transmission, it may tune its transmission parameters to access the channel. Yet, it should continue sensing the spectrum every T seconds in order to vacate the channel if the primary user reappears. This is due to the fact that sensing a channel and transmitting in the same channel can not be done simultaneously. The sensing period T determines the maximum time that the secondary user disregards the primary user activity and may impose harmful interference on the legacy network. Therefore, the choice of T

forces a delay on the primary transmission and hence a degradation of the quality of service (QoS). On the other hand, a larger value of T increases the secondary system's opportunity to access the underutilized spectrum. The selection of T should depend on the type of the primary service and should be set by the regulator.

Thus, we divide the primary services into two general regimes in terms of their sensitivity to transmission delay; 1) *Small-Period* regimes in which the frequency of primary users reappearance is high, forcing T to be chosen relatively small (e.g. WiMAX networks), and 2) *Large-Period* regimes in which larger T may be tolerated since the reappearance of the primary signals occurs on a longer time scale (e.g. DVB-T applications).

Fig. 2.3 represents the frame structure considered for the periodic spectrum sensing. Each frame consists of one sensing slot τ and one data transmission slot $T - \tau$. For a given sensing time τ , the number of samples used for sensing of one subchannel is $M = \tau f_s$ where f_s is the sensing sampling frequency in all subchannels.

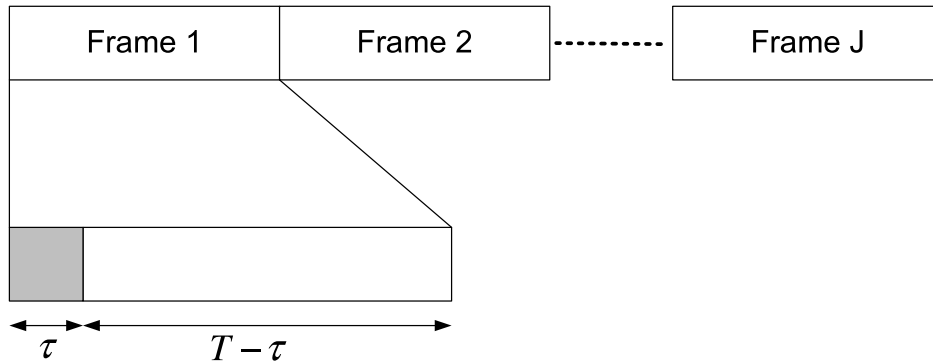


Fig. 2.3. The frame structure of periodic spectrum sensing.

2.3 Summary

In this chapter, we first explained some background on signal detection for spectrum sensing and then presented the general system model used in this study.

Chapter 3

Wideband Spectrum Sensing With Uniform Channel Sensing Durations[†]

In this chapter, we first present the complementary system model and then review the relevant features of the received primary signals and consider their detection in each subchannel. This leads to the introduction of the proposed wideband spectrum sensing framework. We also present a low-complexity and efficient algorithm for implementing the proposed wideband spectrum sensing framework.

3.1 Primary Communication

Here, we consider a multicarrier modulation-based primary communication system over the wideband spectrum. Multiuser orthogonal frequency division multiplexing (OFDM) is a great candidate for such scenario since it has been recognized as an excellent candidate for high data rate transmission over wideband channels and makes the *subband* manipulation easy and clear.

[†]This chapter has been accepted for publication in part in *IEEE Transactions on Signal Processing* [42], and has been presented in part in *Proceedings of IEEE International Conference on Communications (ICC'10)* [43].

3.1.1 Received Primary Signals

We consider a multipath fading channel in which $h(l), l = 0, 1, \dots, L - 1$ represents the discrete time channel response between the primary transmitter and the secondary user where L denotes the number of resolvable paths. Considering $s(n)$ as the transmitted primary signal (with the cyclic prefix), the received signal at the secondary receiver is given by

$$r(n) = \sum_{l=0}^{L-1} h(l)s(n-l) + w(n) \quad (3.1)$$

where $w(n)$ is additive complex white Gaussian noise (AWGN) with zero mean and variance σ_w^2 i.e., $w(n) \sim \mathcal{CN}(0, \sigma_w^2)$. In fading environments, since the multipath delay spread is comparable to the transmitted signal duration, the wideband wireless channel exhibits frequency selectivity [44] and its frequency response is represented as

$$H_k = \frac{1}{\sqrt{N}} \sum_{n=0}^{L-1} h(n)e^{-j2\pi nk/N}, \quad k = 1, 2, \dots, N \quad (3.2)$$

where $N \geq L$. By taking advantage of the cyclic prefix in OFDM signals, the N -point discrete Fourier transform (DFT) of the received signal can be decomposed as

$$R_k = \frac{1}{\sqrt{N}} \sum_{n=0}^{N-1} r(n)e^{-j2\pi nk/N} = H_k S_k + W_k, \quad k = 1, 2, \dots, N \quad (3.3)$$

where S_k is the primary transmitted signal at subchannel k and W_k is the N -point DFT of the received noise, $w(n)$. It can be shown that $W_k \sim \mathcal{CN}(0, \sigma_w^2)$. We assume that the channel is slowly fading such that $\{H_k\}_{k=1}^N$ are constant during the detection interval. We assume the transmitted signal S_k , the channel response H_k , and the noise W_k to be mutually independent.

Since cognitive radio is initially proposed to be exploited for a fixed wireless network in the TV channels, it is reasonable to assume that the channel conditions between the primary and the secondary users are slowly fading such that they can be assumed to be fixed for the period of interest [6]. This assumption is also valid for OFDM multicarrier systems [44]. In our sensing framework, the only information that the secondary user needs to know is the noise power density σ_w^2 and the channel

coefficients between the primary user and secondary user $\{H_k\}$. The noise variance σ_w^2 can easily be obtained when measuring the power level of a channel which is known to be idle. For example, TV channel 37 in the US is currently idle and not being exploited [45]. The channel coefficients $\{H_k\}$ can also be obtained *a priori* when the primary transmitter is known for sure to be active. This *a priori* information about the channel condition is attainable since most of the TV stations and OFDM systems transmit pilot signals periodically for this specific purpose.

3.1.2 Signal Detection in Each Subchannel

After decomposing the received signal into N different waveforms, we are able to independently perform the sensing task in each individual subband. Consequently, we perform signal detection in each subchannel to be used for the joint detection framework. Thus, sensing each subchannel k can be formulated as a binary hypothesis test as following,

$$\begin{aligned} \mathcal{H}_{0,k} &: R_k = W_k, & k = 1, 2, \dots, N \\ \mathcal{H}_{1,k} &: R_k = H_k S_k + W_k, & k = 1, 2, \dots, N. \end{aligned} \quad (3.4)$$

where $\mathcal{H}_{0,k}$ denotes the absence of the primary signal in k -th subchannel and $\mathcal{H}_{1,k}$ denotes its presence. As a common method for detecting unknown signals, energy detection for each subband is performed. The decision statistics of the k -th subchannel can be written as

$$T_k = \frac{1}{M} \sum_{m=1}^M |R_k(m)|^2, \quad k = 1, 2, \dots, N \quad (3.5)$$

where M , as defined before, is the number of received samples in each subband. Note that the number of samples, $M = \tau f_s$, is a common factor in all subchannels due to the fact that the sensing time τ is dedicated for sensing the whole wideband channel. The same number of samples for all subchannels owes to the nature of the wideband primary signal considered here. Accordingly, the decision rule is given by

$$T_k \underset{\mathcal{H}_{0,k}}{\overset{\mathcal{H}_{1,k}}{\gtrless}} \varepsilon_k \quad k = 1, 2, \dots, N \quad (3.6)$$

where ε_k is the decision threshold in subband k . We define the received signal-to-noise ratio (SNR) of the k -th subchannel as

$$\gamma_k = \frac{\mathbb{E}[|S_k|^2] |H_k|^2}{\sigma_w^2} \quad (3.7)$$

in which $\mathbb{E}[\cdot]$ denotes expectation. For the sake of brevity, we assume that all primary signals are complex-valued phase-shift-keying (PSK) signals. For a large number of samples (e.g. $M > 40$), we shall use the central limit theorem (CLT) [40] to approximate the cumulative distribution function (CDF) of T_k as a normal distribution under both hypotheses, i.e.,

$$T_k(r) \sim \begin{cases} \mathcal{N}(\sigma_w^2, \sigma_w^4/M), & \text{under } \mathcal{H}_{0,k} \\ \mathcal{N}(\sigma_w^2(\gamma_k + 1), \sigma_w^4(2\gamma_k + 1)/M), & \text{under } \mathcal{H}_{1,k}. \end{cases} \quad (3.8)$$

Accordingly, the probability of false alarm $P_f^{(k)}(\varepsilon_k, M)$ and the probability of detection $P_d^{(k)}(\varepsilon_k, M)$ for the k -th subchannel are given as

$$P_f^{(k)}(\varepsilon_k, \tau) = Pr(T_k > \varepsilon_k | \mathcal{H}_{0,k}) = Q\left(\left(\frac{\varepsilon_k}{\sigma_w^2} - 1\right) \sqrt{\tau f_s}\right) \quad (3.9)$$

and

$$P_d^{(k)}(\varepsilon_k, \tau) = Pr(T_k > \varepsilon_k | \mathcal{H}_{1,k}) = Q\left(\left(\frac{\varepsilon_k}{\sigma_w^2} - \gamma_k - 1\right) \sqrt{\frac{\tau f_s}{2\gamma_k + 1}}\right) \quad (3.10)$$

in which $Q(\cdot)$ denotes the complementary distribution function of the standard Gaussian distribution, defined in [41].

In the context of sensing algorithms, one of the design criteria is to make the probability of false alarm P_f^\ddagger as low as possible since it measures the percentage of vacant channels which are misclassified as busy ones. On the other hand, in order to limit the probability of interfering with primary users, it is desired to keep the probability of missed detection $P_m = 1 - P_d$ low, with P_d given in (3.10).

The threshold ε_k is a tradeoff factor between the probabilities of false alarm and missed detection; a low threshold value will result in high false alarm probability in

[‡]The subscript k is omitted when referring to a generic function.

favor of low missed detection probability and vice versa. Alternatively, the choice of the number of samples M is a tradeoff between the quality and speed of sensing. By increasing the number of samples (the sensing time), the test decision is more accurate but the available time for cognitive radio transmission is reduced, in consequence.

3.2 Optimal Multiband Sensing-Time-Adaptive Joint Detection Framework

In this section, we propose the multiband sensing-time-adaptive joint detection (MSJD) framework, within which we find the detection thresholds $\{\varepsilon_k\}_{k=1}^N$ and the sensing time τ so as to optimize the performance of the secondary network while protecting the primary network at its desired level. Fig. 3.1 illustrates the MSJD framework.

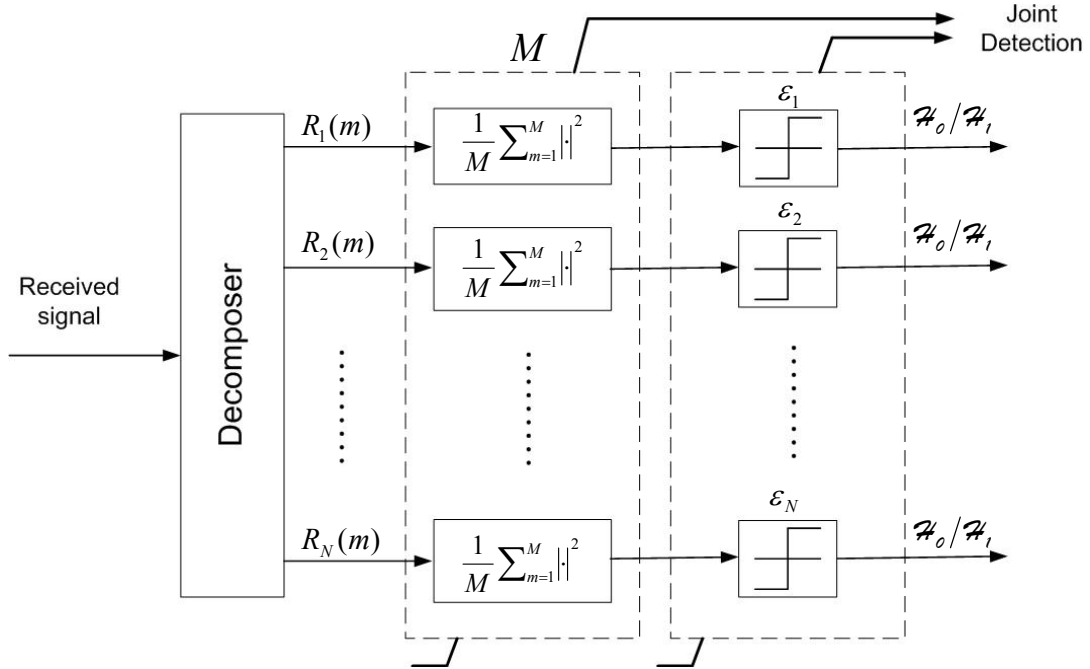


Fig. 3.1. The multiband sensing-time-adaptive joint detection framework for wideband spectrum sensing.

3.2.1 Problem Formulation

In a vector-based format, the probabilities of false alarm and detection are represented as

$$\mathbf{P}_f(\boldsymbol{\varepsilon}, \tau) = \left[P_f^{(1)}(\varepsilon_1, \tau), \dots, P_f^{(N)}(\varepsilon_N, \tau) \right]^T \quad (3.11)$$

and

$$\mathbf{P}_d(\boldsymbol{\varepsilon}, \tau) = \left[P_d^{(1)}(\varepsilon_1, \tau), \dots, P_d^{(N)}(\varepsilon_N, \tau) \right]^T \quad (3.12)$$

in which $\boldsymbol{\varepsilon} = [\varepsilon_1, \varepsilon_2, \dots, \varepsilon_N]^T$ denotes the threshold vector.

To formulate the problem, let r_k denote the opportunistic throughput of the secondary user at subchannel k when it operates in the absence of the primary users and $\mathbf{r} = [r_1, r_2, \dots, r_N]^{\S}$. Recall that $1 - P_f^{(k)}$ represents the percentage of spectrum vacancies detected by the cognitive user and $(T - \tau)/T$ represents the portion of the frame duration available for opportunistic transmission. Hence, we define the available throughput as

$$R(\boldsymbol{\varepsilon}, \tau) = \left(\frac{T - \tau}{T} \right) \mathbf{r}^T (\mathbf{1} - \mathbf{P}_f(\boldsymbol{\varepsilon}, \tau)) \quad (3.13)$$

where $\mathbf{1}$ denotes the all-ones vector. Intuitively, one would like to maximize the opportunistic secondary throughput, $R(\cdot)$.

For a given frame duration T and threshold vector $\boldsymbol{\varepsilon}$, the larger the sensing time τ , the shorter the available time for data transmission $(T - \tau)$ and on the contrary, the larger the probability of opportunities detection $(1 - P_f)$. Hence, we observe that there is an inherent trade-off in the sensing time in the available throughput. On the other hand, for a given sensing time τ , maximizing $R(\boldsymbol{\varepsilon}, \tau)$ results in a large probability of missed detection P_m and large interference with primary users. As a result, the interference to primary users must be constrained (bounded).

In the case of wideband spectrum sensing, the effect of interference on the primary network can be characterized by assigning some relative interference protection priorities over the N subchannels. In particular, we define c_k as the cost of interfering with a primary user in the k -th subchannel and $\mathbf{c} = [c_1, c_2, \dots, c_N]$. In other

^{\S}If the channel gains between secondary users and the transmitter power are known, \mathbf{r} can easily be estimated, exploiting the Shannon capacity formula [44].

words, c_k is interpreted as the relative priorities of the subchannels from the primary network perspective. Consequently, the aggregate interference to primary network is defined as

$$I(\boldsymbol{\varepsilon}, \tau) = \sum_{k=1}^N c_k P_m^{(k)}(\varepsilon_k, \tau). \quad (3.14)$$

A special cases where all subchannels are equally important from the primary users' viewpoint, we may have $c_k = 1$, for all $k = 1, 2, \dots, N$.

The objective of the proposed joint spectrum sensing framework is to jointly optimize the threshold vector $\boldsymbol{\varepsilon}$ and the sensing time τ so as to maximize the available throughput of the secondary user while keeping the weighted interference with primary users below a desired level. Mathematically, the optimization problem can be stated as

$$\max_{\boldsymbol{\varepsilon}, \tau} \quad R(\boldsymbol{\varepsilon}, \tau) \quad (\text{P3.1})$$

$$\text{s. t.} \quad I(\boldsymbol{\varepsilon}, \tau) \leq \xi \quad (\text{C3.1})$$

$$\mathbf{P}_m(\boldsymbol{\varepsilon}, \tau) \preceq \boldsymbol{\alpha} \quad (\text{C3.2})$$

$$\mathbf{P}_f(\boldsymbol{\varepsilon}, \tau) \preceq \boldsymbol{\beta} \quad (\text{C3.3})$$

$$\tau \leq \tau_{\max} \quad (\text{C3.4})$$

where ξ denotes the maximum aggregate interference tolerated by the primary network, $\boldsymbol{\alpha} = [\alpha_1, \alpha_2, \dots, \alpha_N]$ and $\boldsymbol{\beta} = [\beta_1, \beta_2, \dots, \beta_N]$ are the minimum requirements of each subchannel and τ_{\max} represents the maximum allowable sensing time. More specifically, α_k shows the interference margin required in the k -th subchannel and β_k forces a minimum detection of frequency holes. In order to make the analysis easier, we reformulate the problem as

$$\min_{\boldsymbol{\varepsilon}, \tau} \quad R_{\text{miss}}(\boldsymbol{\varepsilon}, \tau) \quad (\text{P3.2})$$

where

$$R_{\text{miss}}(\boldsymbol{\varepsilon}, \tau) = \mathbf{r}^T \left[\mathbf{P}_f(\boldsymbol{\varepsilon}, \tau) \left(1 - \frac{\tau}{T} \right) + \mathbf{1} \frac{\tau}{T} \right] \quad (3.15)$$

is a non-negative value and can be interpreted as the opportunistic throughput loss due to the inherent limitation of sensing. Note that the constraints are the same as the ones in (P3.1).

3.2.2 Minimum Value of Sensing Time τ

Before solving the optimization problem (P3.2), we explore a hidden lower bound on the sensing time τ , denoted τ_{\min} . More specifically, we derive the minimum sensing time τ required to meet the constraints (C3.1)-(C3.3). That is, the least possible sensing time needed to satisfy the expectation of all individual subchannels is derived in this section. This investigation is motivated by several factors. First, we gain valuable insight into the range of values that an optimum value of τ can assume. Second, we make use of τ_{\min} in Section 3.2.4 to solve the problem (P2) for a special range of values of frame duration, T .

For further investigation, we need to extract the relation between the probabilities of false alarm and missed detection. As a rule of thumb, in order to calculate τ_{\min} , we fix the probability of false alarm vector at its maximum tolerable value β . From equations (3.9), (3.10) and for a given probability of false alarm at subchannel k , β_k , the probability of missed detection $P_m^{(k)}(\tau)$ is shown to be

$$P_m^{(k)}(\tau) = Q\left(\frac{1}{\sqrt{2\gamma_k + 1}}\left(\sqrt{\tau f_s \gamma_k} - Q^{-1}(\beta_k)\right)\right). \quad (3.16)$$

Consequently, the minimum sensing time τ_{\min} is calculated as

$$\begin{aligned} \tau_{\min} &= \operatorname{argmin} \tau & (P3.3) \\ \text{s. t.} \quad & \sum_{k=1}^N c_k P_m^{(k)}(\tau) \leq \xi \\ & P_m^{(k)}(\tau) \leq \alpha_k, \quad k = 1, 2, \dots, N. \end{aligned}$$

3.2.3 Convex Optimization

In general, it is difficult to find the global solution for problem (P3.2) since both objective and constraint functions are nonconvex, thus a suboptimal solution is indicated for many cases. However, we observe that this problem can be considered in the convex optimization category under some practical conditions. Consequently, we present the following results, to take advantage of the convexity of problem (P2).

Lemma 1. *The function $P_f^{(k)}(\varepsilon_k, \tau)$ is convex in ε_k and τ if $P_f^{(k)}(\varepsilon_k, \tau) \leq Q(1/\sqrt{3})$.*

Proof. To prove this result, we compute the Hessian matrix as,

$$c_k \times \begin{bmatrix} \left(\frac{\varepsilon_k}{\sigma_w^2} - 1\right) \frac{\tau^2 f_s}{\sigma_w^2} & \frac{\tau f_s}{2} \left(\frac{\varepsilon_k}{\sigma_w^2} - 1\right)^2 - \frac{1}{2} \\ \frac{\tau f_s}{2} \left(\frac{\varepsilon_k}{\sigma_w^2} - 1\right)^2 - \frac{1}{2} & \frac{\left(\frac{\varepsilon_k}{\sigma_w^2} - 1\right)}{4\sigma_w^{-2}\tau} + \frac{\left(\frac{\varepsilon_k}{\sigma_w^2} - 1\right)^3 f_s}{4\sigma_w^{-2}} \end{bmatrix} \quad (3.17)$$

where $c_k = \frac{\sqrt{f_s}}{\sqrt{\tau}\sigma_w^3\sqrt{2\pi}} \exp\left(\frac{\tau f_s}{2} \left(\frac{\varepsilon_k}{\sigma_w^2} - 1\right)^2\right)$. The trace of the matrix is easily shown to be positive. Its determinant can be simplified as

$$\text{Det}(\cdot) = c_k^2 \times \left(\frac{3}{4} \left(\frac{\varepsilon_k}{\sigma_w^2} - 1\right)^2 \tau f_s - \frac{1}{4}\right) \quad (3.18)$$

which is a non-negative value if

$$\left(\frac{\varepsilon_k}{\sigma_w^2} - 1\right) \sqrt{\tau f_s} \geq \frac{1}{\sqrt{3}}. \quad (3.19)$$

As a consequence, the matrix is positive semi-definite, implying that $P_f^{(k)}(\varepsilon_k, \tau)$ is convex under the stated condition. \square

Lemma 2. *The function $P_m^{(k)}(\varepsilon_k, \tau)$ is convex in ε_k and τ if $P_m^{(k)}(\varepsilon_k, \tau) \leq Q(1/\sqrt{3})$.*

Proof. Similar to the proof of Lemma 1, it can be shown that $P_d^{(k)}(\varepsilon_k, \tau)$ is concave, hence $P_m^{(k)}(\varepsilon_k, \tau) = 1 - P_d^{(k)}(\varepsilon_k, \tau)$ is a convex function. \square

Lemma 3. *The function $\left[P_f^{(k)}(\varepsilon_k, \tau) \left(1 - \frac{\tau}{T}\right) + \frac{\tau}{T}\right]$ is convex in ε_k and τ if $P_f^{(k)}(\varepsilon_k, \tau) \leq Q(1/\sqrt{3})$ and $\tau/T \leq 0.5$.*

Proof. To prove this result, we compute the Hessian matrix as,

$$\begin{bmatrix} \left(1 - \frac{\tau}{T}\right) \frac{\partial^2 P_f^{(k)}}{\partial \varepsilon_k^2} & \left(1 - \frac{\tau}{T}\right) \frac{\partial^2 P_f^{(k)}}{\partial \varepsilon_k \partial \tau} - \frac{1}{T} \frac{\partial P_f^{(k)}}{\partial \varepsilon_k} \\ \left(1 - \frac{\tau}{T}\right) \frac{\partial^2 P_f^{(k)}}{\partial \varepsilon_k \partial \tau} - \frac{1}{T} \frac{\partial P_f^{(k)}}{\partial \varepsilon_k} & \left(1 - \frac{\tau}{T}\right) \frac{\partial^2 P_f^{(k)}}{\partial \tau^2} - \frac{2}{T} \frac{\partial P_f^{(k)}}{\partial \tau} \end{bmatrix} \quad (3.20)$$

which is shown to be positive semi-definite for $\tau/T \leq 0.5$ and

$$\left(\frac{\varepsilon_k}{\sigma_w^2} - 1\right) \sqrt{\tau f_s} \geq \frac{1}{\sqrt{3}} \quad (3.21)$$

implying that $\left[P_f^{(k)}(\varepsilon_k, \tau) \left(1 - \frac{\tau}{T} \right) + \frac{\tau}{T} \right]$ is convex under the stated conditions. \square

Recall that a nonnegative weighted sum of convex functions is a convex function [39]. Hence, the objective and constraint functions of problem (P3.2) are convex if the conditions

$$0 \leq \alpha_k \leq Q(1/\sqrt{3}), \quad k = 1, 2, \dots, N \quad (3.22a)$$

$$0 \leq \beta_k \leq Q(1/\sqrt{3}), \quad k = 1, 2, \dots, N \quad (3.22b)$$

$$0 \leq \tau_{\max} \leq 0.5 T \quad (3.22c)$$

are satisfied. Given all these facts, we conclude that the problem (P3.2) is convex if the conditions (3.22) are imposed. This implies that finding the global optimum of (P3.2) is possible, using some efficient numerical search algorithms such as the interior-point method [39]. The conditions given in (3.22) are of practical interest, since a very efficient use of spectrum holes is forced while imposing a very small interference on primary users and keeping the sensing overhead desirably low.

3.2.4 Large-Period Regimes

Consider the case where the frame duration T is large such that

$$\frac{\tau}{T} \ll 1. \quad (3.23)$$

This case characterizes *large-period* regimes, as briefly described in Section 2.2.2. One may notice that defining the range of T which satisfies (3.23) is dependent on different dynamic parameters, since τ is not a pre-determined value and would be selected during the optimization process. However, it is intuitive that the typical optimal values obtained for τ are not drastically larger than the minimum value τ_{\min} obtained in Section 3.2.2. Simulation results given in Section 3.4 give this indication. As a result, we define the large-period regimes as

$$\tau_{\min}^{\text{norm}} = \frac{\tau_{\min}}{T} < 0.01 \quad (3.24)$$

where $\tau_{\min}^{\text{norm}}$ is interpreted as the normalized minimum sensing time. Consequently, the opportunistic throughput loss defined in (3.15) is approximated as

$$R_{\text{miss}}(\boldsymbol{\varepsilon}, \tau) \simeq \mathbf{r}^T \left[\mathbf{P}_f(\boldsymbol{\varepsilon}, \tau) + \mathbf{1} \frac{\tau}{T} \right]. \quad (3.25)$$

Given (3.25) as the new objective function, the original problem (P3.2) is transformed into a convex optimization problem by a change of variables and a transformation of the objective and constraints. The proposition established in this section is that the conditions under which convexity holds is shown to be much wider than the conditions stated in (3.22). Let $\{\varepsilon'_k\}_{k=1}^N$ and τ' denote the new variables whose relation with the original variables are,

$$\begin{cases} \tau' = \sqrt{\tau f_s} \\ \varepsilon'_k = \frac{\varepsilon_k}{\sigma_w^2} \sqrt{\tau f_s} \end{cases} \quad (3.26)$$

for $k = 1, 2, \dots, N$. By substituting these new variables, the probability of false alarm and detection for subchannel k can be represented respectively as

$$P_f^{(k)}(\varepsilon'_k, \tau') = Q(\varepsilon'_k - \tau') \quad (3.27)$$

and

$$P_d^{(k)}(\varepsilon'_k, \tau') = Q\left(\frac{\varepsilon'_k - (\gamma_k + 1)\tau'}{\sqrt{2\gamma_k + 1}}\right). \quad (3.28)$$

Lemma 4. *The function $P_f^{(k)}(\varepsilon'_k, \tau')$ (respectively, $P_m^{(k)}(\varepsilon'_k, \tau')$) is convex in ε'_k and τ' if $P_f^{(k)}(\varepsilon'_k, \tau') \leq 0.5$ (respectively $P_m^{(k)}(\varepsilon'_k, \tau') \leq 0.5$).*

Proof. To prove this lemma, we compute the Hessian matrix of $P_f^{(k)}(\varepsilon'_k, \tau')$ as

$$\nabla^2 Q(\varepsilon'_k - \tau') = \frac{\exp(-(\varepsilon'_k - \tau')^2/2)}{\sqrt{2\pi}} \times (\varepsilon'_k - \tau') \times \begin{bmatrix} 1 \\ -1 \end{bmatrix} \times \begin{bmatrix} 1 \\ -1 \end{bmatrix}^T \quad (3.29)$$

which is semi-definite matrix if $(\varepsilon'_k - \tau') \geq 0$. This means that $P_f^{(k)}(\varepsilon'_k, \tau')$ is convex if $P_f^{(k)}(\varepsilon'_k, \tau') \leq 0.5$. Following the same approach, it can be shown that $P_m^{(k)}(\varepsilon'_k, \tau')$ is also convex if $P_m^{(k)}(\varepsilon'_k, \tau') \leq 0.5$. \square

Accordingly, we conclude that the objective and constraint functions of the problem (P3.2) are convex given the conditions,

$$0 \leq \alpha_k \leq 0.5, \quad k = 1, 2, \dots, N \quad (3.30a)$$

$$0 \leq \beta_k \leq 0.5, \quad k = 1, 2, \dots, N. \quad (3.30b)$$

These ranges of probabilities are particularly interesting from the practical viewpoint since they cover a wider range compared to the conditions given in (3.22).

3.2.5 Multiband Joint Detection Framework

As explained before, we point out that the proposed MSJD framework offers a substantial performance improvement when comparing to the previously proposed multiband joint detection (MJD) framework for wideband spectrum sensing. Here, we explain the MJD framework in more detail. We also distinguish the proposed MSJD framework from the MJD framework and further explain its specific features and properties.

In the MJD framework, the authors haven't considered the periodic sensing scheme and have assumed that the number of samples M (i.e. the sensing time τ) is a constant value and has nothing to do with the optimization process. Accordingly, they have defined the available opportunistic throughput as

$$R(\boldsymbol{\varepsilon}) = \sum_{k=1}^N r_k \left(1 - P_f^{(k)}(\varepsilon_k)\right) \quad (3.31)$$

with $P_f^{(k)}(\varepsilon_k)$ defined in (3.9). Note that $R(\boldsymbol{\varepsilon})$ is a function of the threshold vector $\boldsymbol{\varepsilon}$ only. Based on this definition, they have formulated the optimization problem as

$$\begin{aligned} \max_{\boldsymbol{\varepsilon}} \quad & R(\boldsymbol{\varepsilon}) & (P3.4) \\ \text{s. t.} \quad & I(\boldsymbol{\varepsilon}) \leq \xi \\ & \mathbf{P}_m(\boldsymbol{\varepsilon}) \preceq \boldsymbol{\alpha} \\ & \mathbf{P}_f(\boldsymbol{\varepsilon}) \preceq \boldsymbol{\beta}. \end{aligned}$$

with the same parameters defined in (P3.1). They have further shown that the optimization problem (P3.4) is convex if the conditions given in (3.30) are satisfied.

Although it represents a remarkable advancement in wideband sensing, the MJD framework can be considered as a simplified version of the proposed MSJD framework in which some essential facts and potential system models have not been exploited. The following considerations are noticeable when comparing our framework with the MJD framework:

1- It is indeed crucial to sense the channel periodically since the spectrum must be vacated when a primary user reappears [34]–[38], a feature missing from the MJD framework. In our framework, we modeled the periodic sensing in Section 2.2.2 which effectively takes the primary user integrity into account.

2- Due to the wireless channel fluctuations and fading effects, it is essential to dynamically balance the quality and speed of sensing through an adaptive selection of the sensing time, which is assumed to be fixed in MJD. In our framework, the sensing time τ is considered to be an optimization variable and will wisely and adaptively be chosen so as to compensate both the primary network and secondary user preferences.

3- Considering a unified framework in which the sensing time τ and individual detector parameters (i.e. the decision thresholds, $\{\varepsilon_k\}_{k=1}^N$) are jointly optimized is mandatory for designing a maximally effective cognitive radio network. This consideration is also well-adopted in our framework.

The given considerations are consequently shown to dramatically improve the overall sensing performance in Section 3.4.

3.3 Efficient Implementation of the Multiband Sensing-Time-Adaptive Joint Detection Framework

In this section, some analytical results for solving the original problem (P3.1) are presented. The results are further exploited for presentation of the proposed algorithm which is a two-fold process. First, assuming that the sensing time τ is

constant which classifies the multiband joint detection framework, we present an efficient algorithm for calculating the optimal threshold vector $\boldsymbol{\varepsilon}$. Then, taking advantage of the given algorithm, we propose another efficient algorithm for solving the original multiband sensing-time-adaptive joint detection framework in which $\boldsymbol{\varepsilon}$ and τ are both optimization variables.

3.3.1 Constant τ

Here, we consider the case where τ is a pre-determined value and unrelated to the optimization process. Accordingly, by simplifying both the objective and constraint functions, it is seen that this case has the same framework as multiband joint detection and the optimization problem (P3.1) is transformed into (P3.4). Taking advantage of the monotonicity of the Q -function, (P3.4) is further simplified to

$$\min_{\boldsymbol{\varepsilon}} \quad R_{\text{miss}}(\boldsymbol{\varepsilon}) = \sum_{k=1}^N r_k P_f^{(k)}(\varepsilon_k) \quad (\text{P3.5})$$

$$\text{s.t.} \quad I(\boldsymbol{\varepsilon}) \leq \xi \quad (\text{C3.5})$$

$$\varepsilon_{k,\min} \leq \varepsilon_k \leq \varepsilon_{k,\max}, \quad k = 1, 2, \dots, N \quad (\text{C3.6})$$

where

$$\varepsilon_{k,\max} = \sigma_w^2 \left[\frac{\sqrt{2\gamma_k + 1}}{\sqrt{\tau f_s}} Q^{-1}(1 - \alpha_k) + \gamma_k + 1 \right] \quad (3.32)$$

is the maximum detection threshold that can be chosen in subband k based on α_k given in the constraint (C3.2) and

$$\varepsilon_{k,\min} = \sigma_w^2 \left[\frac{Q^{-1}(\beta_k)}{\sqrt{\tau f_s}} + 1 \right] \quad (3.33)$$

determines the minimum tolerable threshold value which is chosen so as to satisfy the constraint (C3.3). Note that the main difference between (P3.4) and (P3.5) is that the nonlinear constraints (C3.2) and (C3.3) are transformed into the linear constraint (C3.6). Recall that the problem (P3.5) is a convex optimization problem if the conditions given in (3.30) are applied. Therefore, it is possible to find the global optimal solution using numerical methods such as the interior-point method. However, in order to have a more insightful view of the optimization process and

to solve the optimization problem with less complexity, we propose an optimal algorithm which quickly and efficiently computes the optimal threshold vector.

3.3.2 Dual Problem

In order to further explore the optimization problem (P3.5), we take advantage of the Lagrangian duality properties presented in [39]. Consequently, we define the Lagrangian of the problem (P3.5) as

$$L(\boldsymbol{\varepsilon}, \lambda_1, \boldsymbol{\lambda}_2, \boldsymbol{\lambda}_3) = \mathbf{r}^T \mathbf{P}_f(\boldsymbol{\varepsilon}) + \lambda_1(I(\boldsymbol{\varepsilon}) - \xi) + \boldsymbol{\lambda}_2^T(\boldsymbol{\varepsilon} - \boldsymbol{\varepsilon}_{\max}) + \boldsymbol{\lambda}_3^T(-\boldsymbol{\varepsilon} + \boldsymbol{\varepsilon}_{\min}) \quad (3.34)$$

where $\lambda_1, \boldsymbol{\lambda}_2 = [\lambda_2^{(1)}, \lambda_2^{(2)}, \dots, \lambda_2^{(N)}]$ and $\boldsymbol{\lambda}_3 = [\lambda_3^{(1)}, \lambda_3^{(2)}, \dots, \lambda_3^{(N)}]$ are non-negative Lagrangian dual variables associated with the constraint functions. Accordingly, the Lagrangian dual function is defined as

$$g(\lambda_1, \boldsymbol{\lambda}_2, \boldsymbol{\lambda}_3) = \inf_{\boldsymbol{\varepsilon}} L(\boldsymbol{\varepsilon}, \lambda_1, \boldsymbol{\lambda}_2, \boldsymbol{\lambda}_3). \quad (3.35)$$

Recall that the dual function is a lower bound on the optimal solution of the problem (P3.5), \bar{p} , which is achieved by the primal optimal variable $\bar{\boldsymbol{\varepsilon}}$. That is, the inequality $g(\lambda_1, \boldsymbol{\lambda}_2, \boldsymbol{\lambda}_3) \leq \bar{p}$ holds for any $\lambda_1 \geq 0, \boldsymbol{\lambda}_2 \succeq 0$ and $\boldsymbol{\lambda}_3 \succeq 0$. Consequently, the dual optimization problem is defined as

$$\begin{aligned} \max. \quad & g(\lambda_1, \boldsymbol{\lambda}_2, \boldsymbol{\lambda}_3) \\ \text{s. t.} \quad & \lambda_1 \geq 0, \boldsymbol{\lambda}_2 \succeq 0, \boldsymbol{\lambda}_3 \succeq 0 \end{aligned} \quad (3.36)$$

which is formulated to reduce the gap between the optimal solution \bar{p} and the Lagrangian function $g(\lambda_1, \boldsymbol{\lambda}_2, \boldsymbol{\lambda}_3)$. Denote the optimal solution of the dual problem (3.36) as \bar{d} which is achievable by the optimal dual variables $\bar{\lambda}_1, \bar{\boldsymbol{\lambda}}_2$ and $\bar{\boldsymbol{\lambda}}_3$, i.e. $\bar{d} = g(\bar{\lambda}_1, \bar{\boldsymbol{\lambda}}_2, \bar{\boldsymbol{\lambda}}_3)$. Since the original problem (P3.5) is convex and Slater's condition is satisfied, strong duality holds for this problem which means that the duality gap $\bar{p} - \bar{d}$ is zero [39] and consequently, any primal and dual optimal variables $\bar{\boldsymbol{\varepsilon}}, \bar{\lambda}_1, \bar{\boldsymbol{\lambda}}_2$ and $\bar{\boldsymbol{\lambda}}_3$ must satisfy the Karush-Kuhn-Tucker (KKT) conditions

$$I(\bar{\varepsilon}) \leq \xi \quad (\text{K3.1})$$

$$\varepsilon_{k,\min} \leq \bar{\varepsilon}_k \leq \varepsilon_{k,\max}, \quad k = 1, 2, \dots, N \quad (\text{K3.2})$$

$$\bar{\lambda}_1 \geq 0, \quad \bar{\lambda}_2 \succeq 0, \quad \bar{\lambda}_3 \succeq 0 \quad (\text{K3.3})$$

$$\bar{\lambda}_1 (I(\bar{\varepsilon}) - \xi) = 0 \quad (\text{K3.4})$$

$$\bar{\lambda}_2^{(k)} (\bar{\varepsilon}_k - \varepsilon_{k,\max}) = 0, \quad k = 1, 2, \dots, N \quad (\text{K3.5})$$

$$\bar{\lambda}_3^{(k)} (-\bar{\varepsilon}_k + \varepsilon_{k,\min}) = 0, \quad k = 1, 2, \dots, N \quad (\text{K3.6})$$

$$\nabla L(\bar{\varepsilon}, \bar{\lambda}_1, \bar{\lambda}_2, \bar{\lambda}_3) = \mathbf{0}. \quad (\text{K3.7})$$

On the other hand, given the fact that the primal problem is convex, satisfying the KKT conditions is *sufficient* for finding the primal and dual optimal points. That is, any primal and dual variables $\bar{\varepsilon}$, $\bar{\lambda}_1$, $\bar{\lambda}_2$ and $\bar{\lambda}_3$ set which satisfies the KKT conditions is the optimal solution and results in zero duality gap. Before refining the KKT conditions, we need the following Lemma.

Lemma 5. *If $I(\varepsilon_{\max}) \geq \xi$, then the objective function of the problem (P3.5) is minimized if $I(\varepsilon) = \xi$.*

Proof. In order to prove this Lemma, we first show that

$$\frac{1}{c_k} \frac{dR_{\text{miss}}}{dP_m^{(k)}} \leq 0, \quad k = 1, 2, \dots, N. \quad (3.38)$$

We define $t_k = \left(\frac{\varepsilon_k}{\sigma_w^2} - \gamma_k - 1\right) \sqrt{\tau f_s}$. In line with proving the inequality (3.38), we have

$$\frac{dP_f^{(k)}}{d\varepsilon_k} = \frac{-\sqrt{\tau f_s}}{\sqrt{2\pi}} \exp\left(-\frac{(t_k + \gamma_k \sqrt{\tau f_s})^2}{2}\right)$$

and

$$\frac{dP_m^{(k)}}{d\varepsilon_k} = \frac{\sqrt{\tau f_s}}{\sqrt{2\pi}(2\gamma_k + 1)} \exp\left(-\frac{t_k^2}{2(2\gamma_k + 1)}\right). \quad (3.39)$$

Therefore, it follows

$$\frac{dP_f^{(k)}}{dP_m^{(k)}} = \frac{dP_f^{(k)}}{d\varepsilon_k} \frac{1}{\frac{dP_m^{(k)}}{d\varepsilon_k}} = -\sqrt{2\gamma_k + 1} \exp\left(\frac{(t_k + \gamma_k \sqrt{\tau f_s})^2}{2} - \frac{t_k^2}{2(2\gamma_k + 1)}\right) \leq 0. \quad (3.40)$$

Thus, it can be shown that

$$\frac{1}{c_k} \frac{dR_{\text{miss}}}{dP_m^{(k)}} = \frac{r_k}{c_k} \frac{dP_f^{(k)}}{dP_m^{(k)}} \leq 0, \quad k = 1, 2, \dots, N. \quad (3.41)$$

The inequality (3.38) shows that, $R_{\text{miss}}(\boldsymbol{\varepsilon})$ is decreasing in all components of $I(\boldsymbol{\varepsilon})$, so the objective function of the problem (P3.3) is minimized if the aggregate interference $I(\boldsymbol{\varepsilon})$ is set to its maximum value ξ . \square

According to Lemma 5, it is seen that condition (K3.1) is an equality constraint rather than an inequality constraint. Moreover, condition (K3.4) is satisfied for any $\bar{\lambda}_1 \geq 0$ and thus, it can be eliminated from (K3). In order to solve the remaining KKT conditions, we start with extracting the condition (K3.7) as

$$r_k \frac{dP_f^{(k)}}{d\bar{\varepsilon}_k} + \bar{\lambda}_1 c_k \frac{dP_m^{(k)}}{d\bar{\varepsilon}_k} + \bar{\lambda}_2^{(k)} - \bar{\lambda}_3^{(k)} = 0, \quad k = 1, \dots, N. \quad (K3.8)$$

Denoting

$$\bar{t}_k = \left(\frac{\bar{\varepsilon}_k}{\sigma_w^2} - \gamma_k - 1 \right) \sqrt{\tau f_s} \quad (3.42)$$

as the transformed primal variable, we can re-write (K3.8) as

$$\begin{aligned} & -r_k \frac{\sqrt{\tau f_s}}{\sqrt{2\pi}} \exp\left(\frac{-(\bar{t}_k + \gamma_k \sqrt{\tau f_s})^2}{2}\right) \\ & + \bar{\lambda}_1 c_k \frac{\sqrt{\tau f_s}}{\sqrt{2\pi}(2\gamma_k + 1)} \exp\left(\frac{-\bar{t}_k^2}{2(2\gamma_k + 1)}\right) + \bar{\lambda}_2^{(k)} - \bar{\lambda}_3^{(k)} = 0 \end{aligned} \quad (K3.9)$$

which is a nonlinear equation in multiple variables and is very difficult to solve. Generally, there is no conventional method for solving KKT conditions and only a few special cases result in a closed-form solution. In our problem, since the KKT conditions (K3.1) and (K3.7) are non-linear equations, finding a closed-form solution is extremely difficult and thus, a numerical algorithm is indicated.

3.3.3 Efficient Algorithm for the Multiband Joint Detection

Here, we would like to find the optimal primal and dual parameters $\bar{\varepsilon}$, $\bar{\lambda}_1$, $\bar{\lambda}_2$ and $\bar{\lambda}_3$ by satisfying the KKT conditions given in (K3). Aiming to further simplify the problem, we first assume that all the optimal thresholds $\{\bar{\varepsilon}_k\}_{k=1}^N$ lie strictly

between the specified maximum and minimum values, i.e. $\varepsilon_{k,\min} < \bar{\varepsilon}_k < \varepsilon_{k,\max}$ for all k . In other words, we assume that the condition (K3.2) is valid even if the equality is removed. This assumption may not be generally valid and some of the thresholds must assume the boundary values in order to satisfy all the KKT conditions. However, for the interim, we present results based on the aforementioned assumption and will deal with the boundary thresholds in the next stages of the algorithm. Based on the assumption, it is seen that $\bar{\lambda}_2^{(k)}$ and $\bar{\lambda}_3^{(k)}$ are zero for all $k = 1, \dots, N$ according to conditions (K3.5)-(K3.6). As a result, only the exponential factors remain in condition (K3.9), i.e., we have

$$\exp\left(\frac{0.5\bar{t}_k^2}{2\gamma_k + 1} - \frac{(\bar{t}_k + \gamma_k\sqrt{\tau f_s})^2}{2}\right) = \frac{\bar{\lambda}_1 c_k}{r_k\sqrt{2\gamma_k + 1}}. \quad (3.43)$$

After taking the logarithms of both sides of the equation and doing some simplifications, (3.43) is transformed into

$$\left(\bar{t}_k + \frac{\sqrt{\tau f_s}}{2} + \gamma_k\sqrt{\tau f_s}\right)^2 = -\frac{2\gamma_k + 1}{\gamma_k} \log\left(\frac{\bar{\lambda}_1 c_k}{r_k\sqrt{2\gamma_k + 1}}\right) + \frac{\tau f_s}{4}(2\gamma_k + 1). \quad (3.44)$$

Generally, equation (3.44) has two solutions, but only one of them is valid for our problem as can easily be shown using (3.33). Substituting (3.42) in (3.44), we can write the detection threshold $\bar{\varepsilon}_k$ as

$$\bar{\varepsilon}_k = \sigma_w^2 \left[\frac{1}{2} + \sqrt{\frac{2\gamma_k + 1}{\gamma_k} \left[\frac{-1}{\tau f_s} \log\left(\frac{\bar{\lambda}_1 c_k}{r_k\sqrt{2\gamma_k + 1}}\right) + \frac{\gamma_k}{4} \right]} \right] \quad (3.45)$$

which is a closed-form function of $\bar{\lambda}_1$. Having such a function enables us to substitute (3.45) into the KKT condition (K3.1) and obtain the optimal $\bar{\lambda}_1$. Note that equation (K3.1) is an equality condition and can easily be solved using various fast and efficient numerical root-finding methods such as the Newton-Raphson method, fixed point iteration method, etc. Once $\bar{\lambda}_1$ is obtained, the detection thresholds $\{\bar{\varepsilon}_k\}_{k=1}^N$ are accordingly obtained. Note that these computed threshold values are optimal only if they satisfy the assumption of strictly lying between the specified values, i.e. $\varepsilon_{k,\min} < \bar{\varepsilon}_k < \varepsilon_{k,\max}$ for all $k = 1, \dots, N$, since the other KKT conditions are easily shown to be satisfied. That is, if some of the computed threshold values

$\{\bar{\varepsilon}_k\}_{k=1}^N$ take values outside of the admissible range $[\varepsilon_{k,\min}, \varepsilon_{k,\max}]$, it means that neither is the solution optimal nor is the assumption of $\bar{\lambda}_2$ and $\bar{\lambda}_3$ being zero valid. This means that, there might be some $\{\bar{\lambda}_2^{(k)}\}_{k=1}^N$ (or $\{\bar{\lambda}_3^{(k)}\}_{k=1}^N$) which must have non-zero values and accordingly, the associated thresholds must take the boundary values $\{\varepsilon_{k,\min}\}_{k=1}^N$ (or $\{\varepsilon_{k,\max}\}_{k=1}^N$). This fact is easily concluded from the KKT conditions (K3.5)-(K3.6).

Generally, there is no way to know which $\{\bar{\lambda}_2^{(k)}\}_{k=1}^N$ (or $\{\bar{\lambda}_3^{(k)}\}_{k=1}^N$) are non-zero and in the worst case an exhaustive search may be needed. However, we observe that once a specific subset of $\{\bar{\lambda}_2^{(k)}\}_{k=1}^N$ (or $\{\bar{\lambda}_3^{(k)}\}_{k=1}^N$) are known to be non-zero (say, for example, the subset S_p), then the thresholds associated with S_p must take the boundary values $\varepsilon_{k,\min}$ (or $\varepsilon_{k,\max}$). Consequently, equation (3.45) and a modified version of equation (K3.1) can be written for the remaining $\{\bar{\varepsilon}_k\}_{k=1}^N - S_p$ primal variables and, accordingly, the optimal $\bar{\lambda}_1$ can be computed. Therefore, if S_p is determined, the problem can easily be solved. Given this, the main question is how to determine S_p . One possible and naive algorithm is to iteratively search for different scenarios. That is, in each iteration we assume a subset of $\{\bar{\varepsilon}_k\}_{k=1}^N$ contains the boundary value and consequently compute the remaining variables. We stop the iteration when all the thresholds satisfy condition (K3.2). The main problem with this strategy is that its complexity is very high and increases exponentially with the number of primal variables N . In the worst case, the number of iterations is $2^{(N+1)}$ which is undesirable when the number of subchannels is relatively large. In order to decrease the complexity, we propose an efficient algorithm which finds the optimal solution with much lower complexity.

To present the algorithm, we first exploit the fact that $\bar{\varepsilon}_k$ is a monotonically non-increasing function of $\bar{\lambda}_1$ according to (3.45). This property allows us to specify a maximum and minimum value for $\bar{\lambda}_1$ in each subchannel k based on KKT condition (K3.2). Thus, we can define

$$\bar{\lambda}_{1,\max(\min)}^{(k)} = \frac{r_k \sqrt{2\gamma_k + 1}}{c_k} \times \exp \left(\frac{-\gamma_k \tau f_s}{2\gamma_k + 1} \left(\frac{\varepsilon_{k,\min(\max)}^2}{\sigma_w^4} + \frac{\varepsilon_{k,\min(\max)}}{\sigma_w^2} - \frac{\gamma_k}{2} \right) \right) \quad (3.46)$$

as the maximum (minimum) value associated with $\bar{\lambda}_1$ in the k -th subchannel. Note that these values are obtained under the assumption that $\bar{\lambda}_2$ and $\bar{\lambda}_3$ are zero. To

further explain the algorithm, we need the following Lemma.

Lemma 6. *If $\bar{\lambda}_1$ is a known value and has been proved to be the optimal dual Lagrangian variable which satisfies all the conditions (K3), we have*

$$\text{If } \lambda_{1,\min}^{(k)} \leq \bar{\lambda}_1 \leq \lambda_{1,\max}^{(k)} \text{ then } \bar{\lambda}_2^{(k)} = \bar{\lambda}_3^{(k)} = 0 \quad (3.47a)$$

$$\text{If } \bar{\lambda}_1 < \lambda_{1,\min}^{(k)} \text{ then } \bar{\lambda}_2^{(k)} \neq 0 \text{ and } \bar{\lambda}_3^{(k)} = 0 \quad (3.47b)$$

$$\text{If } \bar{\lambda}_1 > \lambda_{1,\max}^{(k)} \text{ then } \bar{\lambda}_2^{(k)} = 0 \text{ and } \bar{\lambda}_3^{(k)} \neq 0 \quad (3.47c)$$

for $k = 1, 2, \dots, N$.

Proof. Lemma 6 can be proved by contradiction. □

According to Lemma 6, if the optimal Lagrangian variable $\bar{\lambda}_1$ is known, then all the optimal detection thresholds can be easily obtained. This is an interesting result which forms the basis of our algorithm. On the other hand, knowing $\lambda_{1,\min}^{(k)}$ and $\lambda_{1,\max}^{(k)}$ for all $k = 1, 2, \dots, N$ as given in (3.46) enables us to partition the $\bar{\lambda}_1 \geq 0$ domain into $2N + 1$ non-overlapping subdomains $\{S_1, S_2, \dots, S_{2N+1}\}$ in which

$$S_i = \{\bar{\lambda}_1 \in \mathbb{Z} \mid A_i \leq \bar{\lambda}_1 < A_{i+1}, A_1 = 0, A_{2N+2} = \infty\} \quad (3.48)$$

determines the i -th subdomain. Basically, A_i is the sorted version of $\{\lambda_{1,\max}^{(k)}, \lambda_{1,\min}^{(k)}\}_{k=1}^N$ which can mathematically be represented as

$$A_i = \operatorname{argmin} \left\{ \bigcup_{k=1}^N \{\lambda_{1,\max}^{(k)}, \lambda_{1,\min}^{(k)}\} - \{A_1, \dots, A_{i-1}\} \right\}. \quad (3.49)$$

An illustrative example in which $N = 6$ subchannels are considered is plotted in Fig. 3.2. As shown in the figure, we can only assume $2N + 1$ different scenarios for any optimal Lagrangian variable $\bar{\lambda}_1$. That is, in each subdomain S_i , only one of the conditions given in Lemma 6 holds for all possible $\bar{\lambda}_1$ in the subdomain S_i . In other words, if $\bar{\lambda}_1$ lies in the i -th subdomain and one specific condition among the ones given in Lemma 6 holds, that condition is valid for all $\bar{\lambda}_1 \in S_i$. Given this fact, Algorithm 3.1 is adopted for solving the problem (P3.5).

As depicted in the algorithm, the maximum number of iterations is $2N + 1$ which means that the iteration-complexity increases linearly with the number of subchan-

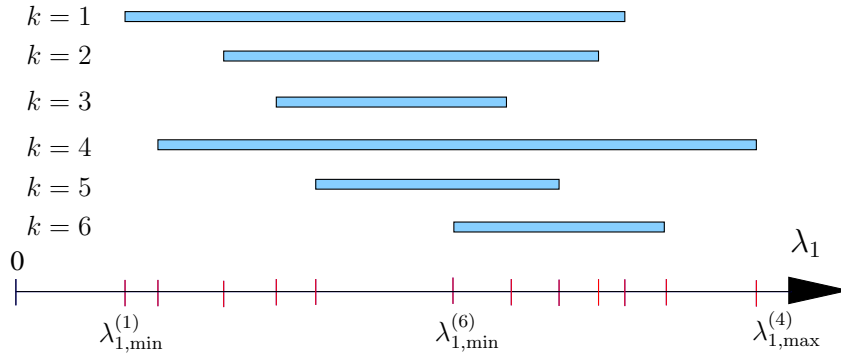


Fig. 3.2. An example of the maximum and minimum values associated with $\bar{\lambda}_1$ in each subchannel k and their mappings to the $\lambda_1 > 0$ axis.

nels, N . Note that the inner loop is only for variable assignment and doesn't add any complexity. In each iteration, only one computation (D_i) is needed whose number of flops[¶] is $2N + 3$. In addition, only one root-finding procedure is required. The complexity is low since the variable of interest $\bar{\lambda}_1$ is one-dimensional. Therefore, it can be concluded that the overall complexity of Algorithm 3.1 is $\mathcal{O}(N^2)$ ^{||}. The complexity is very low when compared to the other commonly used numerical methods such as the barrier method whose complexity is on the order of $N^{3.5}$ (i.e. $\mathcal{O}(N^{3.5})$) [39], particularly when the number of subchannels is large which is usually the case in practice. Although Algorithm 3.1 is specifically designed for solving the optimization problem (P3.5), it can be easily generalized to a wide range of practical convex optimization problems in different research areas including cognitive radio and wireless communications.

3.3.4 Efficient Algorithm for Multiband Sensing-Time-Adaptive Joint Detection

In this section, we propose an algorithm which computes the optimal detection threshold vector ε and sensing time τ as given in the problem (P3.2). The basic idea is, instead of jointly optimizing the optimization variables, we optimize them in a disjoint two-stage algorithm. In the first stage of the algorithm, we assume that the

[¶]One addition, subtraction, multiplication, or division of two floating point numbers is referred to as a floating-point operation (or flop).

^{||}The notation $\mathcal{O}(\cdot)$ gives a rough estimation of complexity. It is computed by expressing the number of floating-point operations (flops) needed for implementation of the algorithms as a (polynomial) function of the problem dimensions and keeping the leading terms.

Algorithm 3.1 Low-Complexity Implementation of the MJD Framework

Calculate S_i using (3.48)
for $i = 1$ to $2N + 1$ **do**
 for $k = 1$ to N **do**
 if $\lambda_{1,\max}^{(k)} \geq A_{i+1}$ and $\lambda_{1,\min}^{(k)} \leq A_i$ **then**
 Calculate $\bar{\varepsilon}_k(\bar{\lambda}_1)$ using (3.45)
 else if $\lambda_{1,\min}^{(k)} \geq A_{i+1}$ **then**
 $\bar{\varepsilon}_k(\bar{\lambda}_1) = \varepsilon_{k,\max}$
 else if $\lambda_{1,\max}^{(k)} \leq A_i$ **then**
 $\bar{\varepsilon}_k(\bar{\lambda}_1) = \varepsilon_{k,\min}$
 end if
 end for
 $D_i = (I(\bar{\varepsilon}(A_i)) - \xi) \times (I(\bar{\varepsilon}(A_{i+1})) - \xi)$
 if $D_i \leq 0$ **then**
 $\bar{\lambda}_1 \leftarrow$ Solve $I(\bar{\varepsilon}(\bar{\lambda}_1)) = \xi$ for λ_1
 $\bar{\varepsilon} \leftarrow$ Substitute $\bar{\lambda}_1$ in all $\bar{\varepsilon}_k(\bar{\lambda}_1)$
 Break
 end if
end for

sensing time τ is a constant value. Therefore, the original problem is reformulated as the one stated in (P3.5). In the second stage, we update the sensing time τ based on the information obtained from the previous stage. We also use iteration in our algorithm in order to refine the information used in each stage. That is, after completing stage 2, we repeat stage 1 based on the updated sensing time τ obtained from the previous iteration and so on. However, in Section 3.4, it is shown that the number of required iterations is small and, most likely, on the second or third iteration, the optimal solution is obtained.

Since the first stage of the algorithm has already been explained in Section 3.3.3, we focus on the second stage here. In order to implement stage 2, we need some information from the previous stage. We specifically exploit probabilities of missed detection for this purpose. There are four main parameters which are effective in determining probabilities of missed detection $\mathbf{P}_m(\varepsilon, \tau)$. These parameters are the achievable throughput r_k , the interference cost c_k , the channel SNR γ_k and the sensing time τ . This is an intuitive result which can be easily extracted from the objective and constraint functions in the problem (P3.1). To be more specific, equation (C3.1) determines how to assign different values to every $P_m^{(k)}(\cdot)$ based

on the aforementioned four main parameters in order to achieve the maximum secondary aggregate throughput. In other words, these parameters determine the relation of different missed detection probabilities (i.e. their relative proportion) and accordingly equation (C3.1) fixes them to specific values.

Having this fact in mind, we observe that the parameters γ_k , c_k and r_k are channel-dependent values and can vary in each subchannel but the sensing time τ is a global value and is the same in each subchannel. Therefore, we can intuitively conclude that the channel-dependent parameters are more effective in determining the missed detection probabilities than the channel-independent sensing time τ . That is, the relative proportion of different missed detection probabilities is mostly dependent on the parameters which are different in each subchannel rather than the globally constant sensing time τ . On the other hand, it is seen that these so called channel-dependent parameters are fixed values and depend only on the system model. Thus, the computed missed detection probabilities in the first stage will remain almost unchanged even if the sensing time τ changes in the next iteration. We exploit this information to implement the second stage of the algorithm. Accordingly, in the second stage, we assume that probabilities of missed detection are fixed at the values $\hat{P}_m^{(k)}$ obtained from the first stage. Thus, we can write the probability of false alarm as

$$P_f^{(k)}(\tau) = Q\left(\sqrt{2\gamma_k + 1}Q^{-1}(1 - \hat{P}_m^{(k)}) + \sqrt{\tau f_s \gamma_k}\right). \quad (\text{C3.5})$$

Accordingly, the optimization problem is converted to

$$\min_{\tau} R_{\text{miss}}(\tau) = \sum_{k=1}^N r_k \left(\left(1 - \frac{\tau}{T}\right) P_f^{(k)}(\tau) + \frac{\tau}{T} \right) \quad (\text{P3.6})$$

$$\text{s.t.} \quad \mathbf{P}_f(\tau) \preceq \boldsymbol{\beta} \quad (\text{C3.7})$$

which has been proved to be convex if $0 \leq \beta_k \leq 0.5$ [35]. Since the only optimization variable is τ , we can re-write the problem as

$$\min_{\tau} R_{\text{miss}}(\tau) \quad (\text{P3.7})$$

$$\text{s.t.} \quad \tau \geq \text{argmax} \left\{ \tau_{\min}^{(1)}, \tau_{\min}^{(2)}, \dots, \tau_{\min}^{(N)} \right\} \quad (\text{C3.8})$$

Algorithm 3.2 Low-Complexity Implementation of the proposed MSJD Framework

Choose an initial sensing time τ (e.g. $\tau = 2\tau_{\min}$)

$\delta =$ Accuracy threshold

repeat

 Run Algorithm 3.1

$R_{\text{miss}}^{\text{old}} \leftarrow$ Compute $R_{\text{miss}}(\varepsilon, \tau)$

 Calculate $\hat{P}_m^{(k)}$

$\tau \leftarrow$ Solve (P3.7) for τ

$R_{\text{miss}}^{\text{new}} \leftarrow$ Compute $R_{\text{miss}}(\tau)$

until $|R_{\text{miss}}^{\text{new}} - R_{\text{miss}}^{\text{old}}| < \delta$

in which

$$\tau_{\min}^{(k)} = \frac{1}{\gamma_k^2 f_s} \left[Q^{-1}(\beta_k) - \sqrt{2\gamma_k + 1} Q^{-1}(1 - \hat{P}_m^{(k)}) \right]^2 \quad (3.51)$$

is the minimum required sensing time at subchannel k obtained from (3.50). The optimization problem (P3.7) can easily be solved by taking the derivative of the objective function and setting it to zero in order to obtain the optimal value of τ . The calculated τ is the optimal solution if it satisfies the constraint (C3.8), otherwise the boundary value given in (C3.8) is chosen. After solving the problem (P3.7), the second stage of the algorithm is complete and we can repeat the first stage based on the updated value of τ until the solution is accurate enough. However, we intuitively showed that the probabilities of missed detection are not very dependent on the sensing time τ , thus the number of iterations would be very small. As a validation, in Section 3.4, it is shown that on the second or third iteration a very accurate solution is obtained. Therefore, we can conclude that the complexity order of this strategy is the same as the one in Algorithm 3.1 (i.e. $\mathcal{O}(N^2)$). In order to explain the procedures in a unified matter, Algorithm 3.2 is adopted.

3.4 Simulation Results

In this section, computer simulation results are presented to evaluate the proposed spectrum sensing schemes. Consider a primary user communication over a wideband spectrum of 6.4-MHz in which OFDM modulation with 16 subcarriers is adopted (i.e. $N = 16$). Each individual subchannel is characterized by different parameters in which γ_k , r_k , and c_k denote the received SNR, the throughput rate (kbps), and

TABLE 3.1
TYPICAL SYSTEM PARAMETER SET USED FOR THE SIMULATION - WIDEBAND SENSING WITH
UNIFORM CHANNEL SENSING DURATIONS

k	1	2	3	4	5	6	7	8
γ_k	0.38	1.37	0.32	0.24	0.35	0.27	0.39	0.38
r_k (kbps)	857	206	853	900	611	808	561	325
c_k	8.94	1.68	3.81	6.91	9.01	2.07	3.43	3.44
k	9	10	11	12	13	14	15	16
γ_k	0.74	0.37	0.51	0.26	0.31	0.25	0.23	0.81
r_k (kbps)	212	391	219	830	308	650	924	138
c_k	1.79	3.38	1.63	1.66	1.02	3.30	1.98	8.91

the cost coefficient, respectively. Furthermore, in each subchannel k , we assume a minimum primary user protection level of 90%, i.e. $\alpha_k = 0.1$ and an opportunity detection margin of $\beta_k = 0.2$. Moreover, the maximum time for which the secondary network is unaware of the primary activity (i.e. T) is chosen such that $f_s T = 3000$.

3.4.1 Example 1: Multiband Sensing-Time-Adaptive Joint Detection Framework

In this example, we evaluate the multiband sensing-time-adaptive joint detection (MSJD) framework. To make a fair comparison, two schemes are considered here. First, a multiband joint detection (MJD) framework [33] with the same constraints and the number of samples $M = \tau f_s = 150$ is examined. Recall that the MJD framework maximizes the available secondary throughput by a joint optimization of the detection thresholds. Second, an algorithm which searches uniform thresholds to maximize the available throughput within the same framework is studied. One typical parameter set used for simulation is given in Table 3.1.

Fig. 3.3 plots the maximum available throughput for cognitive radio transmission versus the aggregate interference in the primary network. The percentages given in the figure represent the maximum available throughput relative to the maximum ideal throughput which denotes the throughput achieved with no sensing error and zero sensing time (i.e. $\sum_{k=1}^N r_k$). It is evident in the figure that our proposed framework achieves a performance superior to the other approaches. Two main observations are notable here. First, other than the detection thresholds, the sensing

time is a critical parameter which should be dynamically assigned due to the channel fluctuations and fading effects. Second, in order to adjust a intelligent tradeoff between the available throughput and interference to the primary user, we need a unified framework which optimizes all of these parameters. These considerations are well adopted in our framework.

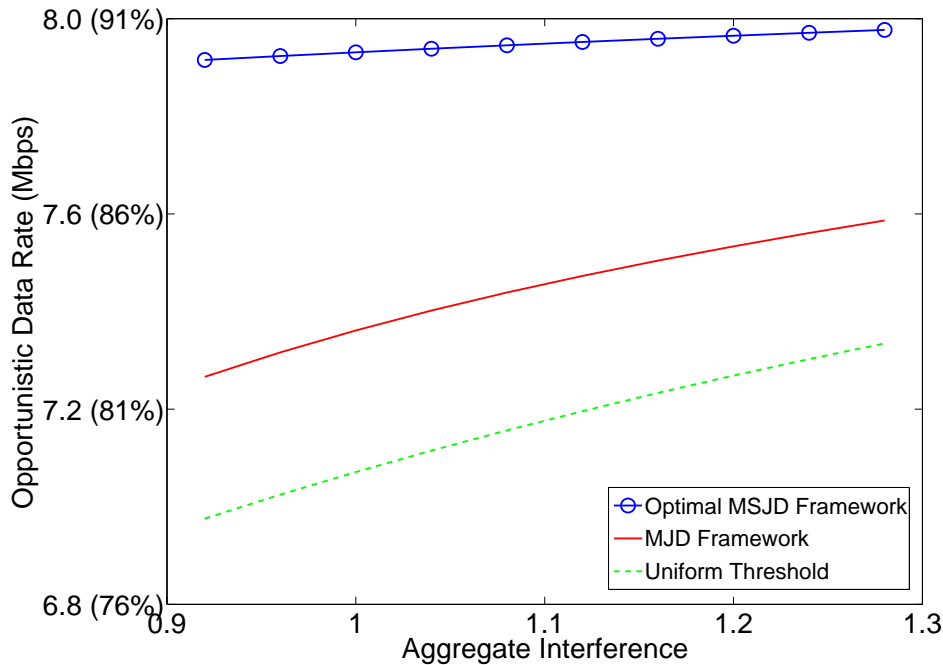


Fig. 3.3. The available opportunistic throughput for cognitive radio transmission vs. the aggregate interference to the primary network.

In Fig. 3.4, the number of samples M is plotted versus the SNR increment above the γ_k 's listed in Table 3.1. We observe that as the channel condition improves, the optimal number of samples is decreased. This study is interesting since it illustrates the necessity of dynamically assigning the sensing time as opposed to a fixed allocation strategy considered in the MJD algorithm. Moreover, Fig. 3.4 reveals that the minimum number of samples obtained from the constraints is not drastically smaller than the optimal number. This verifies the approximation used in (3.25). Another validation to our approximation is depicted in Fig. 3.5, which shows the available throughput versus the normalized minimum sensing time $\tau_{\min}^{\text{norm}}$. It can be seen that the approximation used in (3.25) becomes more precise as $\tau_{\min}^{\text{norm}}$ decreases.

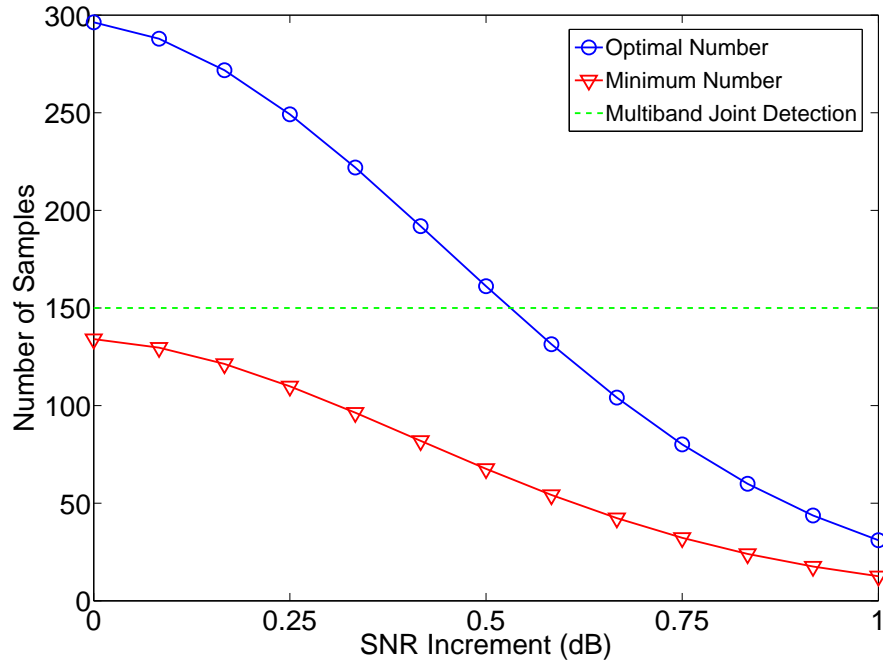


Fig. 3.4. The number of samples vs. the SNR increment (dB) above the SNRs, γ_k , listed in Table 3.1, when the aggregate interference to the primary network $\xi = 1$ and $f_s T = 8000$.

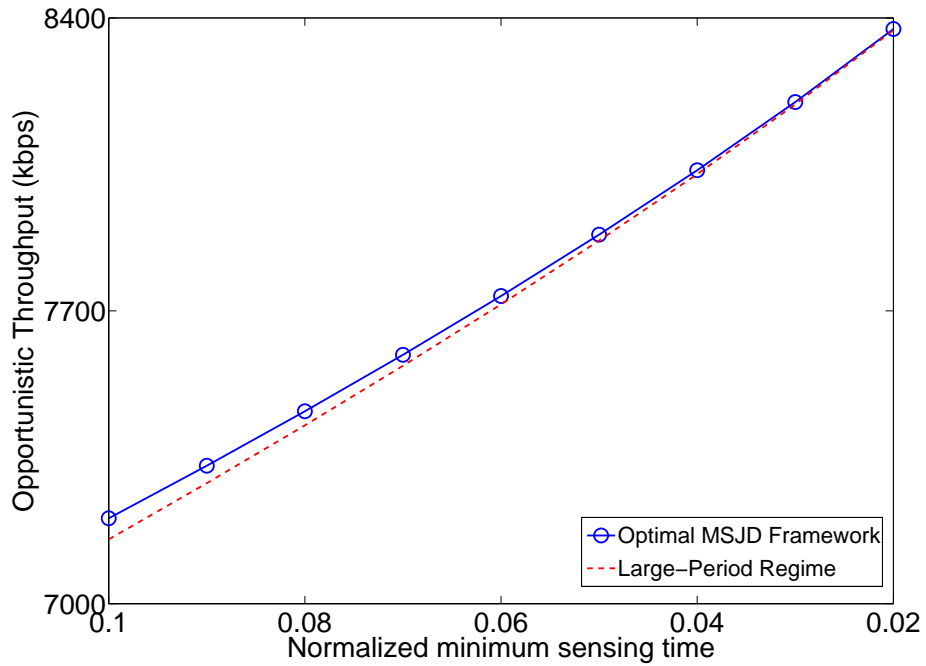


Fig. 3.5. The available opportunistic throughput for cognitive transmission vs. the normalized minimum sensing time $\tau_{\min}^{\text{norm}}$, when the aggregate interference to the primary network $\xi = 1$.

3.4.2 Example 2: Efficient Low-Complexity Wideband Sensing Algorithm

This example studies the optimal algorithms which are proposed for solving both the MSJD and MJD framework. Algorithm 3.1 optimizes the detection threshold vector ε when the sensing time τ is a predetermined value which better suits the MJD framework. Considering the design concerns presented in the MSJD framework, we further developed an optimal iterative algorithm (named as Algorithm 3.2) which computes the optimal values of both the detection threshold vector ε and sensing time τ .

Fig. 3.6 plots the the maximum available throughput for cognitive radio transmission versus the aggregate interference in the primary network. The parameter set used for simulation is the same as the one given in Table 3.1. As depicted in the figure, the optimal solutions can easily be achieved by the proposed algorithms. It should also be noted that only two iterations are used for implementing Algorithm 3.2 which verifies that the required number of iterations is very small.

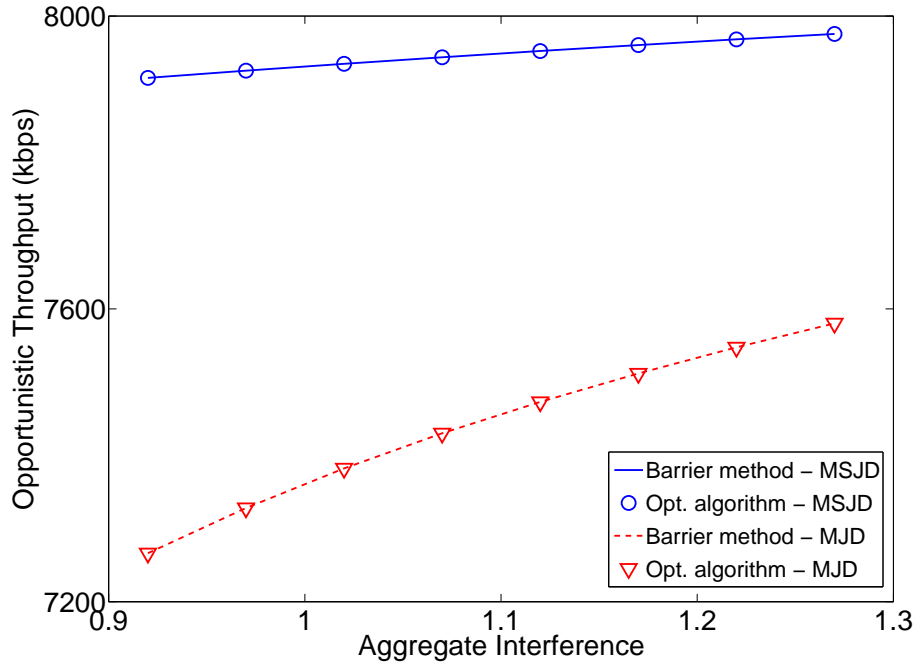


Fig. 3.6. The available opportunistic throughput for cognitive radio transmission vs. the aggregate interference to the primary network.

To demonstrate the efficiency of the proposed algorithms, Fig. 3.7, which roughly compares the implementation complexity of the Algorithm 3.1 with other numerical convex optimization methods, is given. Specifically, Fig. 3.7 plots the average time required for implementing the MJD framework versus the number of narrowband subchannels in the wideband spectrum. The parameters used here are the same as the ones given in Table 3.1. We observe that the average running time of the proposed algorithm is much smaller than the average running time of the other numerical methods, all implemented on the same machine. Although this study is dependent on several factors like the processor speed, the memory capacity, the specific computer code and etc., it gives us a rough and qualitative measure of the implementation complexity. It also proves the efficiency of the proposed algorithm and shows its cost- and time- effectiveness.

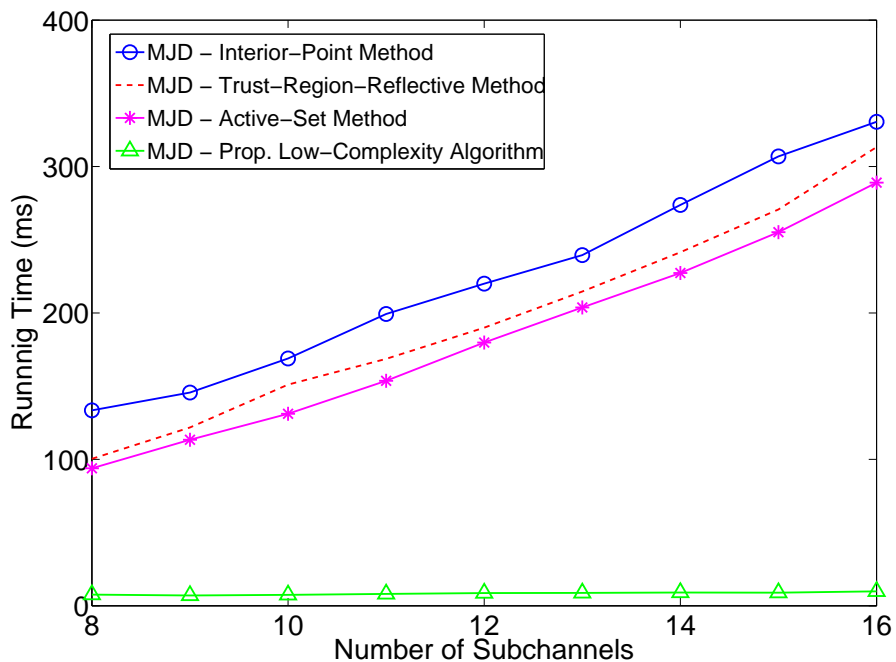


Fig. 3.7. The average running time used for implementation of the MJD framework vs. the number of narrowband subchannels in the wideband spectrum, when the normalized aggregate interference to the primary user $\xi = 1$ and $\|c\| = 15$, where $\|\cdot\|$ denotes Euclidean norm.

In Fig. 3.8, the maximum available throughput for the cognitive transmission is plotted versus the initial number of samples (initial sensing time) given in Algorithm 3.2. In order to present another evaluation of Algorithm 3.1, the number of samples for the MJD framework is set to the given initial number of samples. It is evident

in the figure that we can obtain the optimal solution with running at most three iterations. This is another validation of the small of number of iterations required by Algorithm 3.2. We also observe that the MSJD framework outperforms the MJD framework. The optimized missed detection probabilities in each iteration are depicted in Fig. 3.9 for illustration. This figure shows that the values assigned to missed detection probabilities are almost independent of the number of samples M , which illustrates the procedure exploited in Section 3.3.4.

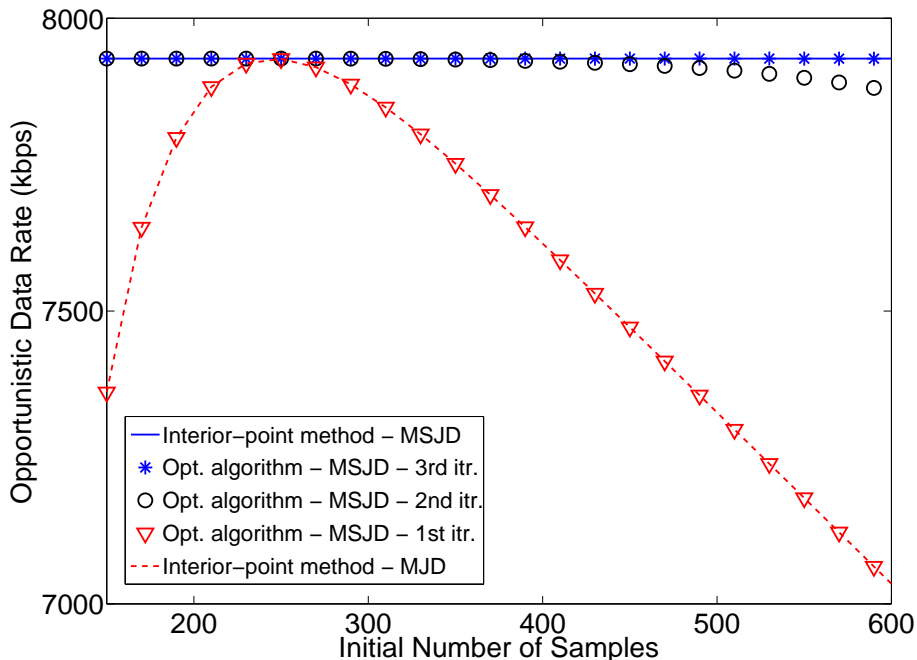


Fig. 3.8. The available opportunistic throughput for cognitive radio transmission vs. the initial number of samples defined in Algorithm 3.2, when the aggregate interference to the primary user $\xi = 1$.

Generally speaking, the simulation results show that the MSJD framework can improve the secondary network capacity while protecting the the primary network from harmful interference, and it can be implemented in practical systems with very low computation (hence implementation) complexity using the proposed algorithms.

3.5 Summary

In this chapter, we first proposed an optimal framework for wideband spectrum sensing with uniform channel sensing durations, referred to as multiband sensing-

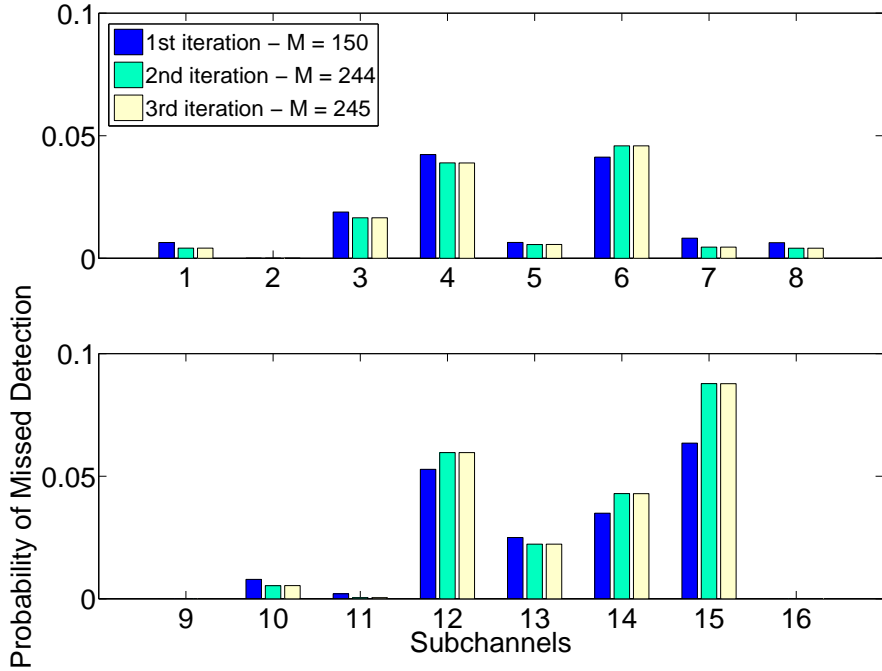


Fig. 3.9. The probability of missed detection obtained in each iteration of Algorithm 3.2, when the aggregate interference to the primary user $\xi = 1$.

time-adaptive joint detection (MSJD). Considering a periodic sensing scheme, we maximized the achievable opportunistic throughput of the secondary user while keeping the interference with the primary network bounded to a reasonably low level. More specifically, we formulated our problem as a joint optimization of the sensing slot duration and individual channel parameters, where the objective function is the throughput capacity of the secondary user and the constraint is the aggregate (weighted) interference to the primary users. Furthermore, we demonstrated that our problem, which is generally non-convex, can be solved as a convex optimization problem if certain practical constraints are imposed.

In addition, we proposed an efficient algorithm which quickly and effectively computes the optimal sensing parameters within the aforementioned MSJD framework. In particular, taking advantage of Lagrangian duality properties presented in [39], we transformed the original optimization problem into a class of equivalent subproblems and solved them accordingly. It was also demonstrated that the computational (hence implementation) complexity of the proposed algorithm is much lower than that of other commonly used numerical approaches such as the interior-

point methods. In particular, we illustrated that the iteration-complexity and the complexity-per-iteration of the proposed algorithm increases linearly as the number of primary individual channels increases. This level of complexity is very interesting from a practical/implementation viewpoint since it is remarkably time- and cost-effective.

Chapter 4

Multichannel Spectrum Sensing With Non-Uniform Channel Sensing Durations[†]

In this chapter, we first present the relevant system model and then review the signal detection in individual subchannels. This leads to the presentation of the sequential multichannel joint detection (SMJD) framework which is well-suited for the case of non-uniform channel sensing durations.

4.1 System Model

Here, we consider a more general primary communication system and assume that the primary wideband received signal is not decomposable and can not be divided into multiple signal waveforms. That is, the multicarrier modulation-based primary system is not the case here, implying that N multiple narrowband signals can not be extracted from the received wideband signal. This means that, instead of capturing the primary wideband signal and decomposing it into multiple narrowband signals, each individual narrowband frequency band[‡] must be sensed separately. On the other hand, in order to collectively consider all the narrowband channels and have

[†]This chapter has been submitted in part to *IEEE Transactions in Communications* [46], and *Proceedings of IEEE International Conference on Communications (ICC'11)* [47], and *Proceedings of IEEE International Conference on Acoustics, Speech and Signal Processing (ICASSP'11)* [48].

[‡]We refer to the “narrowband frequency bands” as “channels”, in subsequent sections.

a more effective sensing framework, the secondary user should sequentially sense N multiple channels during the sensing phase.

4.1.1 Sequential Periodic Sensing

A modified version of the previously presented periodic sensing scheme is considered here. In each sensing frame, there is a sensing phase and a transmission phase. In order to take into account all the narrowband channels, the secondary user should sequentially sense N multiple channels during the sensing phase. Fig. 4.1 represents the frame structure used for the sequential periodic sensing. Each frame consists of a sensing period τ and a transmission period $T - \tau$. The sensing slot τ is divided into N subslots which are assigned for sensing the individual channels. Note that the order of the channels to be sensed is not relevant to the sensing performance. The sensing time duration τ and the sensing subslot durations $\{\tau_k\}_{k=1}^N$ are the sensing design parameters which must be determined. Note that non-uniform channel sensing durations is attainable in this scenario since the channels are sensed separately allowing different sensing time durations $\{\tau_k\}_{k=1}^N$. For a given sensing subslot duration τ_k , the number of samples used for sensing subchannel k is $M_k = \tau_k f_s$, where f_s denotes the sensing sampling frequency.

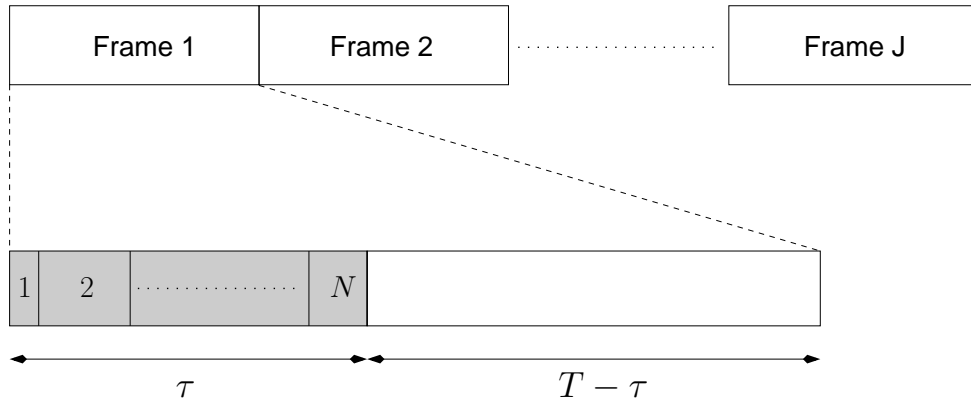


Fig. 4.1. The frame structure of the sequential periodic sensing.

4.1.2 Signal Detection in Each Channel

As explained before, binary hypothesis testing is used for modeling the detection problem on each channel; i.e. we have two hypotheses,

$$\begin{aligned}\mathcal{H}_{0,k} : r_k(n) &= w_k(n), & k &= 1, 2, \dots, N \\ \mathcal{H}_{1,k} : r_k(n) &= h_k s_k(n) + w_k(n), & k &= 1, 2, \dots, N\end{aligned}\quad (4.1)$$

where $r_k(n)$ is the n -th received sample on channel k and h_k denotes the channel response of the k -th narrowband channel, which is regarded as flat fading and assumed to be constant during the sensing period (i.e. slowly fading). Signal $s_k(n)$ represents the n -th symbol transmitted by the primary network over the k -th frequency band and the $w_k(n)$ are independent and identically distributed (i.i.d.) additive noise samples which are assumed to be circularly symmetric complex Gaussian (CSCG) with zero mean and variance σ_w^2 .

Exploiting energy detection, the decision statistic at the k -th channel can be written as

$$T_k(r) = \frac{1}{M_k} \sum_{n=1}^{M_k} |r_k(n)|^2, \quad k = 1, 2, \dots, N \quad (4.2)$$

where M_k , as defined before, represents the number of samples used for sensing the frequency band k . Moreover, we define the received signal-to-noise ratio (SNR) of the k -th channel as

$$\gamma_k = \frac{\mathbb{E}[|s_k|^2] |h_k|^2}{\sigma_w^2} \quad (4.3)$$

in which $\mathbb{E}[\cdot]$ denotes expectation. For the sake of brevity, we also assume that all primary signals are complex-valued phase-shift-keying (PSK) signals. Following the same central limit theorem (CLT) given in section 3.1.2, we approximate the cumulative distribution function (CDF) of $T_k(r)$ as a normal distribution under both hypotheses and compute the probability of false alarm $P_f^{(k)}(\varepsilon_k, \tau_k)$ and the probability of detection $P_d^{(k)}(\varepsilon_k, \tau_k)$ for the k -th channel as

$$P_f^{(k)}(\varepsilon_k, \tau_k) = Pr(T_k > \varepsilon_k | \mathcal{H}_{0,k}) = Q\left(\left(\frac{\varepsilon_k}{\sigma_w^2} - 1\right) \sqrt{\tau_k f_s}\right) \quad (4.4)$$

and

$$P_d^{(k)}(\varepsilon_k, \tau_k) = Pr(T_k > \varepsilon_k | \mathcal{H}_{1,k}) = Q\left(\left(\frac{\varepsilon_k}{\sigma_w^2} - \gamma_k - 1\right) \sqrt{\frac{\tau_k f_s}{2\gamma_k + 1}}\right) \quad (4.5)$$

respectively, where ε_k denotes the decision threshold.

4.2 Optimal Multichannel Spectrum Sensing Framework - Generic Perspective

In this section, we present the “sequential multichannel joint detection” (SMJD) framework, within which we aim to find the optimal sensing parameters $\{\varepsilon_k\}$, $\{\tau_k\}$ [§] and τ to maximize the opportunistic secondary network throughput capacity while limiting the aggregate interference on the primary network. Fig. 4.2 illustrates the MSJD framework.

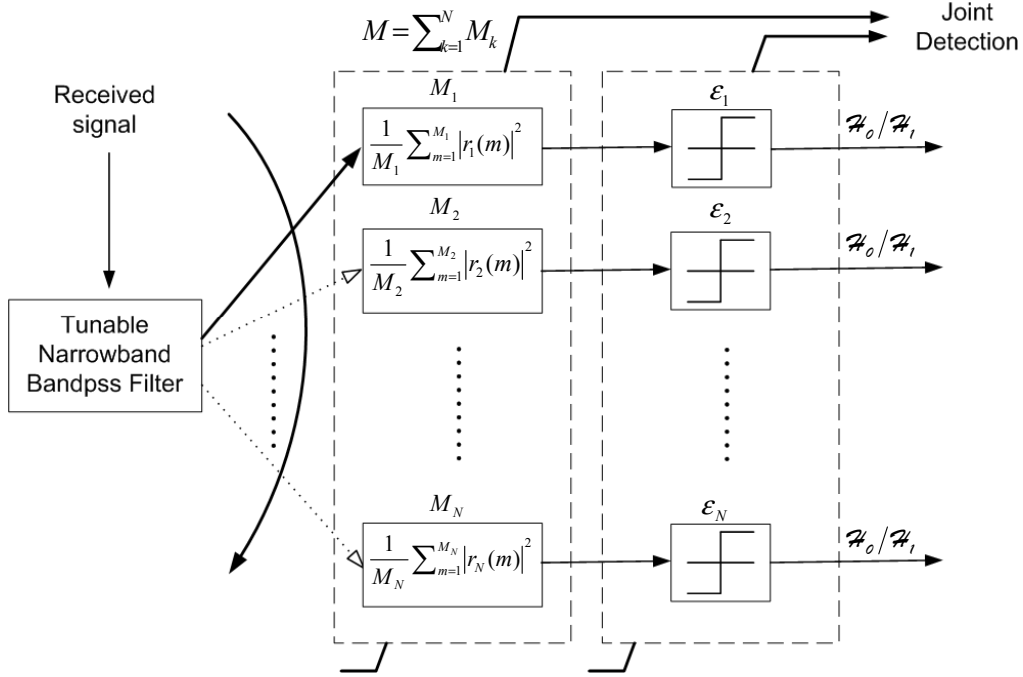


Fig. 4.2. The sequential multiband joint detection framework for multichannel spectrum sensing.

[§]Note that $\{\varepsilon_k\}$ and $\{\tau_k\}$ denote the set $\{\varepsilon_1, \varepsilon_2, \dots, \varepsilon_N\}$ and $\{\tau_1, \tau_2, \dots, \tau_N\}$, respectively.

4.2.1 Problem Formulation

Following the same approach given in Section 3.2.1, let r_k denote the opportunistic throughput of the secondary user over channel k when it operates in the absence of the primary users. Thus, the available opportunistic throughput capacity of the cognitive radio is defined as

$$R(\{\varepsilon_k\}, \{\tau_k\}, \tau) = \left(\frac{T - \tau}{T}\right) \sum_{k=1}^N r_k \left(1 - P_f^{(k)}(\varepsilon_k, \tau_k)\right). \quad (4.6)$$

In the case of multichannel sensing, the effect of interference can also be characterized by assigning some relative interference protection priorities over the N channels. Having c_k as the cost of interfering with a primary user in channel k , the aggregate interference to the primary network is defined as

$$I(\{\varepsilon_k\}, \{\tau_k\}, \tau) = \sum_{k=1}^N c_k P_m^{(k)}(\varepsilon_k, \tau_k). \quad (4.7)$$

Consequently, the optimization problem is formulated as

$$\underset{\{\varepsilon_k\}, \{\tau_k\}, \tau}{\text{maximize}} \quad R(\{\varepsilon_k\}, \{\tau_k\}, \tau) \quad (\text{P4.1})$$

$$\text{subject to} \quad I(\{\varepsilon_k\}, \{\tau_k\}, \tau) \leq \xi \quad (\text{C4.1})$$

$$P_m^{(k)}(\varepsilon_k, \tau_k) \leq \alpha_k, \quad k = 1, 2, \dots, N \quad (\text{C4.2})$$

$$P_f^{(k)}(\varepsilon_k, \tau_k) \leq \beta_k, \quad k = 1, 2, \dots, N \quad (\text{C4.3})$$

$$0 \leq \tau \leq \tau_{\max} \quad (\text{C4.4})$$

$$\sum_{k=1}^N \tau_k = \tau \quad (0 \leq \tau_k \leq \tau, \quad k = 1, 2, \dots, N) \quad (\text{C4.5})$$

where constraint (C4.1) limits the aggregate interference through ξ , and α_k in (C4.2) denotes the maximum probability of missed detection which can be accommodated in channel k . The constraint (C4.3) dictates a minimum opportunistic spectrum utilization of $1 - \beta_k$ in the k -th channel and τ_{\max} in (C4.4) denotes the maximum allowed sensing time. The alternative problem is given as

$$\underset{\{\varepsilon_k\}, \{\tau_k\}, \tau}{\text{minimize}} \quad R_{\text{miss}}(\{\varepsilon_k\}, \{\tau_k\}, \tau) \quad (\text{P4.2})$$

where

$$R_{\text{miss}}(\{\varepsilon_k\}, \{\tau_k\}, \tau) = \sum_{k=1}^N r_k \left(\left(1 - \frac{\tau}{T}\right) P_f^{(k)}(\varepsilon_k, \tau_k) + \frac{\tau}{T} \right) \quad (4.8)$$

is the opportunistic throughput loss. The constraints are the same as the ones in (P4.1).

4.2.2 Minimum Value of Sensing Time τ

Following the same approach given in Section 3.2.2, we derive the minimum sensing time τ which is required to meet the constraints (C4.1)-(C4.5). To do so, we fix the probability of false alarm at its maximum tolerable value β_k , for all $k = 1, 2, \dots, N$. Accordingly, the probability of missed detection $P_m^{(k)}(\tau_k)$ is shown to be

$$P_m^{(k)}(\tau_k) = Q \left(\frac{1}{\sqrt{2\gamma_k + 1}} \left(\sqrt{\tau_k f_s \gamma_k} - Q^{-1}(\beta_k) \right) \right). \quad (4.9)$$

Consequently, the minimum sensing time τ_{\min} is calculated as

$$\begin{aligned} \tau_{\min} &= \operatorname{argmin} \sum_{k=1}^N \tau_k & (P4.3) \\ \text{s. t.} \quad & \sum_{k=1}^N c_k P_m^{(k)}(\tau_k) \leq \xi \\ & P_m^{(k)}(\tau_k) \leq \alpha_k, \quad k = 1, 2, \dots, N. \end{aligned}$$

4.2.3 Convex Optimization

First, we show that the problem (P4.2) can not be solved as a convex optimization.

Lemma 7. *The problem (P4.2) is not a convex optimization problem.*

Proof. In order to prove Lemma 7, we use proof by contradiction. Assume that problem (P4.2) is a convex problem. Then, the objective function $R_{\text{miss}}(\{\varepsilon_k\}, \{\tau_k\}, \tau)$ is convex in $\{\varepsilon_k\}$, $\{\tau_k\}$ and τ . Accordingly, we conclude that the throughput loss function in channel j , $j \in \{1, \dots, N\}$,

$$R_{\text{miss}}^{(j)}(\varepsilon_j, \tau_j, \tau) = r_j \left[\left(1 - \frac{\tau}{T}\right) P_f^{(j)}(\varepsilon_j, \tau_j) + \frac{\tau}{T} \right]$$

which is a three-dimensional function, is also convex in ε_j , τ_j and τ . It can easily be shown that the Hessian matrix of $R_{\text{miss}}^{(j)}(\varepsilon_j, \tau_j, \tau)$ is not positive semi-definite and consequently the function is not convex. This contradicts the initial assumption of $R_{\text{miss}}(\{\varepsilon_k\}, \{\tau_k\}, \tau)$ being convex. Thus, we conclude that the problem (P4.2) is not a *convex* optimization problem. \square

Given Lemma 7, one can conclude that it is very difficult to find the global optimal solution of (P4.2) and consequently a suboptimal solution may be indicated for many cases. However, we observe that it can be made convex under some practical conditions. Specifically, two classes are considered, uniform sensing subslots and non-uniform sensing subslots.

4.2.3.1 Uniform Sensing Subslots

First, we assume that all subslot durations $\{\tau_k\}$ are required to have the same value. That is, the same amount of time must be assigned for sensing each subchannel. This was the case in the *wideband spectrum sensing* investigated in Chapter 3. Given this assumption, we see that $\tau_k = \tau/N$ according to the constraint (C4.5). Accordingly, the optimization problem is simplified to

$$\min_{\{\varepsilon_k\}, \tau} R_{\text{miss}}(\{\varepsilon_k\}, \tau) = \sum_{k=1}^N r_k \left(\left(1 - \frac{\tau}{T}\right) P_f^{(k)}(\varepsilon_k, \tau) + \frac{\tau}{T} \right) \quad (\text{P4.4})$$

where $P_f^{(k)}(\varepsilon_k, \tau)$ is derived by substituting $\tau_k = \tau/N$ in (4.4) and is a function of ε_k and τ only. It is seen that this case simplifies to the “multiband sensing-time-adaptive joint detection” (MSJD) framework, as explained in Section 3.2. It’s been proved that (P4.4) is convex, if the following conditions are satisfied;

$$0 \leq \alpha_k \leq Q(1/\sqrt{3}), \quad k = 1, 2, \dots, N \quad (4.10a)$$

$$0 \leq \beta_k \leq Q(1/\sqrt{3}), \quad k = 1, 2, \dots, N \quad (4.10b)$$

$$0 \leq \tau_{\text{max}} \leq 0.5 T \quad (4.10c)$$

4.2.3.2 Non-Uniform Sensing Subslots

Solving (P4.2) when the subslot durations can be chosen non-uniformly is not straightforward since it is not convex. However, we observe that it can also be transformed into a convex optimization problem by a change of variables and a transformation of the objective and constraints. Let $\{\varepsilon_k^\circ\}$, $\{\tau_k^\circ\}$ and $\hat{\tau}$ denote the new variables whose relation with the original variables are,

$$\begin{cases} \varepsilon_k^\circ = (\frac{\varepsilon_k}{\sigma_w^2} - 1) \\ \tau_k^\circ = (\tau_k f_s) / \tau \\ \hat{\tau} = \tau \end{cases} \quad (4.11)$$

for $k = 1, 2, \dots, N$. Substituting the new variables, the probabilities of false alarm and missed detection for channel k can be represented as

$$P_f^{(k)}(\varepsilon_k^\circ, \tau_k^\circ, \hat{\tau}) = Q\left(\varepsilon_k^\circ \sqrt{\tau_k^\circ \hat{\tau}}\right) \quad (4.12)$$

and

$$P_m^{(k)}(\varepsilon_k^\circ, \tau_k^\circ, \hat{\tau}) = 1 - Q\left((\varepsilon_k^\circ - \gamma_k) \sqrt{\frac{\tau_k^\circ \hat{\tau}}{2\gamma_k + 1}}\right) \quad (4.13)$$

respectively. We apply this transformation to the aggregate interference $I(\{\varepsilon_k\}, \{\tau_k\}, \tau)$ and throughput loss $R_{\text{miss}}(\{\varepsilon_k\}, \{\tau_k\}, \tau)$, as defined in (4.7) and (4.8), respectively.

Consequently, the problem (P4.2) is transformed into

$$\underset{\{\varepsilon_k^\circ\}, \{\tau_k^\circ\}, \hat{\tau}}{\text{minimize}} \quad R_{\text{miss}}(\{\varepsilon_k^\circ\}, \{\tau_k^\circ\}, \hat{\tau}) \quad (\text{P4.5})$$

$$\text{subject to} \quad I(\{\varepsilon_k^\circ\}, \{\tau_k^\circ\}, \hat{\tau}) \leq \xi \quad (\text{C4.6})$$

$$P_m^{(k)}(\varepsilon_k^\circ, \tau_k^\circ, \hat{\tau}) \leq \alpha_k, \quad k = 1, 2, \dots, N \quad (\text{C4.7})$$

$$P_f^{(k)}(\varepsilon_k^\circ, \tau_k^\circ, \hat{\tau}) \leq \beta_k, \quad k = 1, 2, \dots, N \quad (\text{C4.8})$$

$$0 \leq \hat{\tau} \leq \tau_{\text{max}} \quad (\text{C4.9})$$

$$\sum_{k=1}^N \tau_k^\circ = f_s \quad (0 \leq \tau_k^\circ \leq f_s, \quad k = 1, \dots, N). \quad (\text{C4.10})$$

Lemma 8. *The function $P_f^{(k)}(\varepsilon_k^\circ, \tau_k^\circ, \hat{\tau})$ is convex in ε_k° , τ_k° and $\hat{\tau}$ if $P_f^{(k)}(\varepsilon_k^\circ, \tau_k^\circ, \hat{\tau}) \leq Q(1/\sqrt{2})$.*

Proof. To prove Lemma 8, we compute the Hessian matrix as

$$a_k \times \begin{bmatrix} \frac{\dot{\varepsilon}_k \sqrt{\dot{\tau}_k}}{\dot{\tau} \sqrt{\dot{\tau}}} + \frac{\dot{\varepsilon}_k^3 \dot{\tau}_k \sqrt{\dot{\tau}_k}}{\sqrt{\dot{\tau}}} & \frac{-\dot{\varepsilon}_k}{\sqrt{\dot{\tau}_k \dot{\tau}}} + \dot{\varepsilon}_k^3 \sqrt{\dot{\tau}_k \dot{\tau}} & -2\sqrt{\frac{\dot{\tau}_k}{\dot{\tau}}} + 2\dot{\varepsilon}_k^2 \dot{\tau}_k \sqrt{\dot{\tau}_k \dot{\tau}} \\ \frac{-\dot{\varepsilon}_k}{\sqrt{\dot{\tau}_k \dot{\tau}}} + \dot{\varepsilon}_k^3 \sqrt{\dot{\tau}_k \dot{\tau}} & \frac{\dot{\varepsilon}_k \sqrt{\dot{\tau}}}{\dot{\tau}_k \sqrt{\dot{\tau}_k}} + \frac{\dot{\varepsilon}_k^3 \dot{\tau} \sqrt{\dot{\tau}}}{\sqrt{\dot{\tau}_k}} & -2\sqrt{\frac{\dot{\tau}}{\dot{\tau}_k}} + 2\dot{\varepsilon}_k^2 \dot{\tau} \sqrt{\dot{\tau}_k \dot{\tau}} \\ -2\sqrt{\frac{\dot{\tau}_k}{\dot{\tau}}} + 2\dot{\varepsilon}_k^2 \dot{\tau}_k \sqrt{\dot{\tau}_k \dot{\tau}} & -2\sqrt{\frac{\dot{\tau}}{\dot{\tau}_k}} + 2\dot{\varepsilon}_k^2 \dot{\tau} \sqrt{\dot{\tau}_k \dot{\tau}} & 4\dot{\varepsilon}_k \dot{\tau}_k \dot{\tau} \sqrt{\dot{\tau}_k \dot{\tau}} \end{bmatrix}$$

where

$$a_k = \frac{1}{4\sqrt{2\pi}} \exp\left(-\frac{\dot{\varepsilon}_k^2 \dot{\tau}_k \dot{\tau}}{2}\right). \quad (4.14)$$

It can easily be shown that the Hessian matrix is positive semi-definite if $\dot{\varepsilon}_k \sqrt{\dot{\tau}_k \dot{\tau}} \geq 1/\sqrt{2}$. This implies that the function $P_f^{(k)}(\dot{\varepsilon}_k, \dot{\tau}_k, \dot{\tau})$ is convex under the stated condition. \square

Lemma 9. *The function $P_m^{(k)}(\dot{\varepsilon}_k, \dot{\tau}_k, \dot{\tau})$ is convex in $\dot{\varepsilon}_k, \dot{\tau}_k$ and $\dot{\tau}$ if $P_m^{(k)}(\dot{\varepsilon}_k, \dot{\tau}_k, \dot{\tau}) \leq Q(1/\sqrt{2})$.*

Proof. Following the same approach given in the proof of Lemma 8, it can be shown that $P_d^{(k)}(\dot{\varepsilon}_k, \dot{\tau}_k, \dot{\tau})$ is concave, hence $P_m^{(k)}(\dot{\varepsilon}_k, \dot{\tau}_k, \dot{\tau}) = 1 - P_d^{(k)}(\dot{\varepsilon}_k, \dot{\tau}_k, \dot{\tau})$ is a convex function under the stated condition. \square

Lemma 10. *The function $\left[\left(1 - \frac{\dot{\tau}}{T}\right) P_f^{(k)}(\dot{\varepsilon}_k, \dot{\tau}_k, \dot{\tau}) + \frac{\dot{\tau}}{T}\right]$ is convex in $\dot{\varepsilon}_k, \dot{\tau}_k$ and $\dot{\tau}$ if $P_f^{(k)}(\dot{\varepsilon}_k, \dot{\tau}_k, \dot{\tau}) \leq Q(1/\sqrt{2})$ and $\dot{\tau}/T \leq 0.4$.*

Proof. The Hessian matrix is computed as

$$\begin{bmatrix} \left(1 - \frac{\dot{\tau}}{T}\right) \frac{\partial^2 P_f^{(k)}}{\partial \dot{\varepsilon}_k^2} & \left(1 - \frac{\dot{\tau}}{T}\right) \frac{\partial^2 P_f^{(k)}}{\partial \dot{\varepsilon}_k \partial \dot{\tau}_k} & \left(1 - \frac{\dot{\tau}}{T}\right) \frac{\partial^2 P_f^{(k)}}{\partial \dot{\varepsilon}_k \partial \dot{\tau}} - \frac{1}{T} \frac{\partial P_f^{(k)}}{\partial \dot{\varepsilon}_k} \\ \left(1 - \frac{\dot{\tau}}{T}\right) \frac{\partial^2 P_f^{(k)}}{\partial \dot{\varepsilon}_k \partial \dot{\tau}_k} & \left(1 - \frac{\dot{\tau}}{T}\right) \frac{\partial^2 P_f^{(k)}}{\partial \dot{\tau}_k^2} & \left(1 - \frac{\dot{\tau}}{T}\right) \frac{\partial^2 P_f^{(k)}}{\partial \dot{\tau}_k \partial \dot{\tau}} - \frac{1}{T} \frac{\partial P_f^{(k)}}{\partial \dot{\tau}_k} \\ \left(1 - \frac{\dot{\tau}}{T}\right) \frac{\partial^2 P_f^{(k)}}{\partial \dot{\varepsilon}_k \partial \dot{\tau}} - \frac{1}{T} \frac{\partial P_f^{(k)}}{\partial \dot{\varepsilon}_k} & \left(1 - \frac{\dot{\tau}}{T}\right) \frac{\partial^2 P_f^{(k)}}{\partial \dot{\tau}_k \partial \dot{\tau}} - \frac{1}{T} \frac{\partial P_f^{(k)}}{\partial \dot{\tau}_k} & \left(1 - \frac{\dot{\tau}}{T}\right) \frac{\partial^2 P_f^{(k)}}{\partial \dot{\tau}^2} - \frac{2}{T} \frac{\partial P_f^{(k)}}{\partial \dot{\tau}} \end{bmatrix}$$

which is shown to be positive semi-definite if $\dot{\tau}_k/T \leq 2/5$ and $\dot{\varepsilon}_k \sqrt{\dot{\tau}_k \dot{\tau}} \geq 1/\sqrt{2}$. Thus, the function is convex under the given conditions. \square

Note that the equality constraint (C4.10) is linear. Also recall that a non-negative weighted sum of a set of convex functions is also convex [39]. This means

that the objective function and constraints (C4.6)-(C4.9) of problem (P4.5) are convex if conditions

$$0 \leq \alpha_k \leq Q(1/\sqrt{2}), \quad k = 1, 2, \dots, N \quad (4.15a)$$

$$0 \leq \beta_k \leq Q(1/\sqrt{2}), \quad k = 1, 2, \dots, N \quad (4.15b)$$

$$0 \leq \tau_{\max} \leq 0.4 T \quad (4.15c)$$

are satisfied. Given all these facts, we conclude that the problem (P4.5) is convex if the conditions (4.15) are imposed. The conditions given in (4.15) are also of practical interest, since a very efficient use of spectrum holes is forced while imposing a very small interference on primary users and keeping the sensing overhead desirably low.

4.2.4 Large-Period Regimes

Following the same argument given in Section 3.2.4, consider the case where T is large such that $\tau/T \ll 1$ which is mathematically defined as

$$\tau_{\min}^{\text{norm}} = \frac{\tau_{\min}}{T} < 0.01. \quad (4.16)$$

where $\tau_{\min}^{\text{norm}}$ is the normalized minimum sensing time. Likewise, the opportunistic throughput loss defined in (4.8) is approximated as

$$R_{\text{miss}}(\{\varepsilon_k\}, \{\tau_k\}, \tau) \simeq \sum_{k=1}^N r_k \left[P_f^{(k)}(\varepsilon_k, \tau_k) + \frac{\tau}{T} \right] \quad (4.17)$$

which is generally a lower bound to the exact value of $R_{\text{miss}}(\cdot)$, however, in this case, a very tight one. Having (4.17) as the new objective function, we propose that the problem (P4.2) can be solved by convex optimization under much wider conditions compared to the ones given in (4.15). We use the “change of variables” method to transform the problem (P4.2) into a convex problem. Let $\{\varepsilon_k''\}$, $\{\tau_k''\}$ and τ'' denote the new variables whose relation with the original variables are

$$\begin{cases} \varepsilon_k'' = \frac{\varepsilon_k}{\sigma_w^2} \sqrt{\tau_k f_s} \\ \tau_k'' = \sqrt{\tau_k f_s} \\ \tau'' = \tau. \end{cases} \quad (4.18)$$

Accordingly, the probabilities of false alarm and missed detection can be respectively written as

$$P_f^{(k)}(\varepsilon_k'', \tau_k'') = Q(\varepsilon_k'' - \tau_k'') \quad (4.19)$$

and

$$P_m^{(k)}(\varepsilon_k'', \tau_k'') = 1 - Q\left(\frac{\varepsilon_k'' - (\gamma_k + 1)\tau_k''}{\sqrt{2\gamma_k + 1}}\right). \quad (4.20)$$

It can easily be shown that the transformed objective and constraint functions of the problem (P4.2) are convex [¶], under the conditions,

$$0 \leq \alpha_k \leq 0.5, \quad k = 1, 2, \dots, N \quad (4.21a)$$

$$0 \leq \beta_k \leq 0.5, \quad k = 1, 2, \dots, N. \quad (4.21b)$$

4.3 Optimal Multichannel Spectrum Sensing Framework - Decoupled Perspective

4.3.1 Detection Problem

In the previous section, we considered the “sequential multichannel joint detection” (SMJD) framework. Within the framework, we optimized the sensing parameters $\{\varepsilon_k\}$, $\{\tau_k\}$ and τ , so as to maximize the opportunistic secondary throughput given a bound on the aggregate interference imposed on the primary network. Note that in the SMJD framework, the overall interference on the primary network is aggregated into a functional form $I(\{\varepsilon_k\}, \{\tau_k\}, \tau)$. Although the aggregate interference $I(\{\varepsilon_k\}, \{\tau_k\}, \tau)$ is an effective and practical measure of the amount of interference imposed on the primary network, it may not be suitable for some systems.

Recall that we defined some relative priority coefficients in order to characterize the impact of interference induced by the cognitive users. Specifically, we defined

[¶]Refer to the proof of Lemma 4.

c_k as the cost incurred if a primary communication in channel k is interfered with. However, in some situations, it is either difficult or infeasible to define such priority coefficients. That is, transforming the relative priorities assigned to multiple channels into some coefficients might not be possible for certain applications. Therefore, for these applications, interference on each channel should be bounded separately (i.e. independently), making the individual channels partially decoupled. Given this fact, we propose another optimal framework, referred to as “decoupled sequential multichannel joint detection” (D-SMJD), which considers interference on each channel independently. Excluding the aggregate interference from (P4.1), the optimization problem can be written as

$$\underset{\{\varepsilon_k\}, \{\tau_k\}, \tau}{\text{maximize}} \quad R(\{\varepsilon_k\}, \{\tau_k\}, \tau) \quad (\text{P4.6})$$

$$\text{s. t.} \quad P_m^{(k)}(\varepsilon_k, \tau_k) \leq \alpha'_k, \quad k = 1, 2, \dots, N \quad (\text{C4.11})$$

where α'_k is chosen such that the interference to the primary network on channel k is effectively and sufficiently limited. Note that the other constraints (C4.3)-(C4.5) are unchanged and are the same as the constraints in (P4.1). The choice of α'_k also reflects the relative priorities of primary communication in each frequency band. Specifically, α'_k is selected tight enough in order to sufficiently protect each channel according to its priority (i.e. $\alpha'_k \leq \alpha_k$, for all k). As noted before, instead of exploiting the aggregate interference function $I(\{\varepsilon'_k\}, \{\tau'_k\}, \tau')$, we set the boundary values $\{\alpha'_k\}_{k=1}^N$ such that the relative primary interference protection, and effective limitation of the interference to primary users, are accounted for.

To continue further, we use the following result; the proof is omitted due to its similarity to the proof of Lemma 5.

Lemma 11. *The objective function $R(\{\varepsilon_k\}, \{\tau_k\}, \tau)$ in (P4.6) is maximized if $P_m^{(k)}(\varepsilon_k, \tau_k) = \alpha'_k$, for all $k = 1, 2, \dots, N$.*

According to Lemma 11, the probability of false alarm in channel k can be simplified by setting the probability of detection $P_m^{(k)}(\varepsilon_k, \tau_k) = \alpha'_k$, i.e.

$$P_f^{(k)}(\tau_k) = Q\left(\sqrt{2\gamma_k + 1}Q^{-1}(1 - \alpha'_k) + \sqrt{\tau_k f_s \gamma_k}\right) \quad (4.22)$$

is the simplified probability of false alarm which is a function of τ_k only. Since the decision threshold ε_k has been removed from the equation (4.22), we conclude that the individual channels have become partially decoupled. Note that they are still coupled (i.e. dependent) due to the sensing subslot τ_k . According, the optimization problem (P4.6) can be converted to

$$\min_{\{\tau_k\}, \tau} R_{\text{miss}}(\{\tau_k\}, \tau) = \sum_{k=1}^N r_k \left(\left(1 - \frac{\tau}{T}\right) P_f^{(k)}(\tau_k) + \frac{\tau}{T} \right) \quad (\text{P4.7})$$

$$\text{s. t.} \quad P_f^{(k)}(\tau_k) \leq \beta_k, \quad k = 1, 2, \dots, N \quad (\text{C4.12})$$

$$0 \leq \tau \leq \tau_{\max}$$

$$\sum_{k=1}^N \tau_k = \tau \quad (0 \leq \tau_k \leq \tau, \quad k = 1, \dots, N).$$

which is still a non-convex problem. However, we observe that it can also be made convex under some practical conditions.

4.3.2 Convex Optimization

Similar to the study given in Section 4.2.3, we consider two specific classes; uniform sensing subslots and non-uniform sensing subslots.

4.3.2.1 Uniform Sensing Subslots

First, we assume that all subslot durations $\{\tau_k\}$ are required to have the same value which results in $\tau_k = \tau/N$ according to the constraint (C4.5). Accordingly, the optimization problem is simplified to

$$\min_{\tau} R_{\text{miss}}(\tau) = \sum_{k=1}^N r_k \left(\left(1 - \frac{\tau}{T}\right) P_f^{(k)}(\tau) + \frac{\tau}{T} \right) \quad (\text{P4.7})$$

$$\text{s. t.} \quad P_f^{(k)}(\tau) \leq \beta_k, \quad k = 1, 2, \dots, N \quad (\text{C4.13})$$

$$0 \leq \tau \leq \tau_{\max}$$

where $P_f^{(k)}(\tau)$ is derived by substituting $\tau_k = \tau/N$ in (4.22) and is a function of τ only.

Lemma 12. *The function $P_f^{(k)}(\tau)$ as defined in (4.22) is convex in τ if $P_f^{(k)}(\tau) \leq 0.5$ [35].*

Proof. Defining $\delta = \sqrt{2\gamma_k + 1}Q^{-1}(1 - \alpha'_k)$, we have

$$P_f^{(k)}(\tau) = Q\left(\delta + \sqrt{\tau f_s \gamma_k}\right). \quad (4.23)$$

Then, we simply take the second derivative of $P_f^{(k)}(\tau)$ as

$$\begin{aligned} \frac{d^2 P_f^{(k)}}{d\tau^2} &= \frac{d}{d\tau} \left[\frac{-\gamma_k \sqrt{f_s} \tau^{-1/2}}{2\sqrt{2\pi}} \exp\left(-\frac{(\delta + \sqrt{\tau f_s \gamma_k})^2}{2}\right) \right] \\ &= \frac{\tau^{-1} \sqrt{f_s} \gamma_k}{4\sqrt{2\pi}} \left(\tau^{-1/2} + (\delta + \sqrt{\tau f_s \gamma_k}) \sqrt{f_s \gamma_k} \right) \exp(\cdot) \end{aligned} \quad (4.24)$$

which has positive value if $P_f^{(k)}(\tau) \leq 0.5$ and thus $P_f^{(k)}(\tau)$ is convex. We also observe that $P_f^{(k)}(\tau)$ is a monotonically decreasing function under the stated condition. \square

Lemma 13. *The function $R_{\text{miss}}^{(k)} = \left(1 - \frac{\tau}{T}\right) P_f^{(k)}(\tau) + \frac{\tau}{T}$ in τ is convex if $P_f^{(k)}(\tau) \leq 0.5$ [35].*

Proof. Taking the second derivative of $R_{\text{miss}}^{(k)}$, we have

$$\frac{d^2 R_{\text{miss}}^{(k)}}{d\tau^2} = -\frac{2}{T} \frac{dP_f^{(k)}}{d\tau} + \left(1 - \frac{\tau}{T}\right) \frac{d^2 P_f^{(k)}}{d\tau^2} \quad (4.25)$$

which has positive value under the stated condition, this is due to $P_f^{(k)}(\tau)$ being convex and monotonically decreasing. \square

Given all these facts, we conclude that the problem (P4.7) is convex optimization and can be solved efficiently if the following conditions are satisfied;

$$0 \leq \beta_k \leq 0.5, \quad k = 1, 2, \dots, N.$$

4.3.2.2 Non-Uniform Sensing Subslots

Here, we consider the challenging case of “non-uniform sensing subslots” which is the main focus of this chapter. Before examining the problem (P4.7), we point out that a similar sensing problem is studied in [37]. However the development in [37] does

not consider the convexity properties, and, proposes a *bilevel iterative* algorithm for solving the formulated sensing problem. In the first stage (level) it is assumed that τ is a constant value and a transformed version of problem (P4.7), which is convex, is solved. In the next level, the sensing slot τ is updated based on the previous stage.

It is observed that the approach given in [37] is neither simple nor efficient and in most cases the number of iterations for obtaining the optimum solution exploiting this strategy is large. For instance, it has been shown in [37] that the number of iterations could be as large as 1.5×10^5 under some specific conditions. Apart from the iteration complexity, in each iteration, a convex problem must be solved which makes the implementation of the algorithm unwieldy.

Although the problem (P4.7) is generally non-convex, we observe that it can be transformed into a convex optimization problem by a change of variables and a transformation of the objective and constraints. Let $\{\bar{\tau}_k\}_{k=1}^N$ and $\bar{\tau}$ denote the new variables whose relation with the original variables are,

$$\begin{cases} \bar{\tau} = \tau \\ \bar{\tau}_k = \tau_k / \tau \end{cases}$$

for $k = 1, 2, \dots, N$. By substituting these new variables, the probability of false alarm for channel k can be represented as

$$P_f^{(k)}(\bar{\tau}_k, \bar{\tau}) = Q\left(\sqrt{2\gamma_k + 1}Q^{-1}(1 - \alpha'_k) + \sqrt{\bar{\tau}_k \bar{\tau} f_s \gamma_k}\right). \quad (4.26)$$

The throughput loss $R_{\text{miss}}(\{\tau_k\}, \tau)$, as defined in (4.8), is transformed accordingly. The optimization problem (P4.7) can be re-written as

$$\min_{\{\bar{\tau}_k\}, \bar{\tau}} R_{\text{miss}}(\{\bar{\tau}_k\}, \bar{\tau}) \quad (P4.8)$$

$$\text{s. t.} \quad P_f^{(k)}(\bar{\tau}_k, \bar{\tau}) \leq \beta_k, \quad k = 1, 2, \dots, N \quad (C4.14)$$

$$0 \leq \bar{\tau} \leq \tau_{\text{max}} \quad (C4.15)$$

$$\sum_{k=1}^N \bar{\tau}_k = 1 \quad (0 \leq \bar{\tau}_k \leq 1, \quad k = 1, 2, \dots, N). \quad (C4.16)$$

Lemma 14. *The function $P_f^{(k)}(\bar{\tau}_k, \bar{\tau})$ is convex in $\bar{\tau}_k$ and $\bar{\tau}$ if $P_f^{(k)}(\bar{\tau}_k, \bar{\tau}) \leq 0.5$.*

Proof. We simply compute the Hessian matrix as

$$c_k \times \begin{bmatrix} \frac{b_k \sqrt{\bar{\tau}_k}}{\bar{\tau} \sqrt{\bar{\tau}}} + \frac{\bar{\tau}_k \sqrt{\bar{\tau}_k}}{b_k \sqrt{\bar{\tau}}} + \frac{\delta_k \bar{\tau}_k}{\bar{\tau}} & \frac{\sqrt{\bar{\tau} \bar{\tau}_k}}{b_k} - \frac{b_k}{\sqrt{\bar{\tau} \bar{\tau}_k}} + \delta_k \\ \frac{\sqrt{\bar{\tau} \bar{\tau}_k}}{b_k} - \frac{b_k}{\sqrt{\bar{\tau} \bar{\tau}_k}} + \delta_k & \frac{b_k \sqrt{\bar{\tau}}}{\bar{\tau}_k \sqrt{\bar{\tau}_k}} + \frac{\bar{\tau} \sqrt{\bar{\tau}}}{b_k \sqrt{\bar{\tau}_k}} + \frac{\delta_k \bar{\tau}}{\bar{\tau}_k} \end{bmatrix}$$

where

$$c_k = \frac{f_s \gamma_k^2}{4\sqrt{2\pi}} \exp\left(-\frac{(\delta_k + \sqrt{\bar{\tau} \bar{\tau}_k} f_s \gamma_k)^2}{2}\right)$$

$\delta_k = \sqrt{2\gamma_k + 1}Q^{-1}(1 - \alpha'_k)$ and $b_k = 1/(\sqrt{f_s} \gamma_k)$. The trace of the matrix is easily shown to be non-negative. Its determinant can be simplified as

$$\text{Det}(\cdot) = c_k^2 \left(4 + 4 \frac{\delta_k b_k}{\sqrt{\bar{\tau} \bar{\tau}_k}}\right)$$

which is non-negative if $(\delta_k + \sqrt{\bar{\tau} \bar{\tau}_k} f_s \gamma_k) \geq 0$. This means the Hessian matrix is positive semi-definite under the stated condition and hence, the function $P_f^{(k)}(\bar{\tau}_k, \bar{\tau})$ is convex. \square

Lemma 15. *The function $\left[\left(1 - \frac{\bar{\tau}}{T}\right) P_f^{(k)}(\bar{\tau}_k, \bar{\tau}) + \frac{\bar{\tau}}{T}\right]$ is convex in $\bar{\tau}_k$ and $\bar{\tau}$ if $P_f^{(k)}(\bar{\tau}_k, \bar{\tau}) \leq 0.5$ and $\bar{\tau}/T \leq 2/3$.*

Proof. The Hessian matrix is computes as

$$c_k \times \begin{bmatrix} \frac{4b_k}{T} \sqrt{\frac{\bar{\tau}_k}{\bar{\tau}}} + \left(1 - \frac{\bar{\tau}}{T}\right) \frac{1}{c_k} \frac{\partial^2 P_f^{(k)}}{\partial \bar{\tau}^2} & \frac{2b_k}{T} \sqrt{\frac{\bar{\tau}}{\bar{\tau}_k}} + \left(1 - \frac{\bar{\tau}}{T}\right) \frac{1}{c_k} \frac{\partial^2 P_f^{(k)}}{\partial \bar{\tau} \partial \bar{\tau}_k} \\ \frac{2b_k}{T} \sqrt{\frac{\bar{\tau}}{\bar{\tau}_k}} + \left(1 - \frac{\bar{\tau}}{T}\right) \frac{1}{c_k} \frac{\partial^2 P_f^{(k)}}{\partial \bar{\tau} \partial \bar{\tau}_k} & \left(1 - \frac{\bar{\tau}}{T}\right) \frac{1}{c_k} \frac{\partial^2 P_f^{(k)}}{\partial \bar{\tau}_k^2} \end{bmatrix}$$

where

$$c_k = \frac{f_s \gamma_k^2}{4\sqrt{2\pi}} \exp\left(-\frac{(\delta_k + \sqrt{\bar{\tau} \bar{\tau}_k} f_s \gamma_k)^2}{2}\right)$$

$\delta_k = \sqrt{2\gamma_k + 1}Q^{-1}(1 - \alpha'_k)$ and $b_k = 1/(\sqrt{f_s} \gamma_k)$. It can easily be shown that the matrix is positive semi-definite under the stated condition and thus, the function $\left[\left(1 - \frac{\bar{\tau}}{T}\right) P_f^{(k)}(\bar{\tau}_k, \bar{\tau}) + \frac{\bar{\tau}}{T}\right]$ is convex. \square

Given all these results, the problem (P4.8) is convex given the conditions

$$0 \leq \beta_k \leq 0.5, \quad k = 1, 2, \dots, N \quad (4.25a)$$

$$0 \leq \tau_{\max} \leq \frac{2}{3} T \quad (4.25b)$$

which makes it possible to find the optimal solution efficiently [39].

4.4 Simulation Results

In this section, we numerically evaluate the proposed multichannel spectrum sensing frameworks. Consider a cognitive radio system which is to sequentially sense $N = 16$ channels. The maximum time that the secondary user disregards primary activities (i.e. T) is set to 500 *ms*. For each channel, it is expected that opportunistic spectrum utilization is at least 80% (i.e. $\beta_k = 0.2$ for all k) and the primary protection level is $\alpha_k = 0.1$. The sampling frequency and the noise variance are assumed to be $f_s = 25$ KHz and $\sigma_w^2 = 1$, respectively. Other system parameters are given in Table 4.1.

4.4.1 Example 1: Sequential Multichannel Joint Detection Framework

First, we examine the proposed “sequential multichannel joint detection” (SMJD) framework in which the aggregate interference is considered as the constraint. Specifically, two cases are examined here, uniform sensing subslots and non-uniform sensing subslots which were explained in Sections 4.2.3.1 and 4.2.3.2, respectively. While the former characterizes the “multiband sensing-time-adaptive joint detection” (MSJD), the latter refers to the proposed SMJD. To demonstrate the effectiveness of the proposed framework and to make a fair comparison, a “multiband joint detection” (MJD) framework is also examined. Within the MJD framework, the sensing time τ is considered to be fixed in MJD and the subslot durations $\{\tau_k\}$ uniform. For simulation, we assume $\tau = 65$ *ms*.

Fig. 4.3 plots the maximum available throughput for CR transmission versus the aggregate interference on the primary network. The percentages given in the figure represent the maximum available throughput relative to the maximum ideal

TABLE 4.1
TYPICAL SYSTEM PARAMETER SET USED FOR THE SIMULATION - MULTICHANNEL SENSING WITH
NON-UNIFORM CHANNEL SENSING DURATIONS

k	1	2	3	4	5	6	7	8
γ_k	0.38	1.37	0.32	0.24	0.35	0.27	0.39	0.38
r_k (kbps)	857	206	853	900	611	808	561	325
c_k	6.24	1.18	2.67	4.84	6.31	1.45	2.40	2.41
α'_k	0.04	0.06	0.02	0.02	0.03	0.05	0.02	0.04
k	9	10	11	12	13	14	15	16
γ_k	0.74	0.37	0.51	0.26	0.31	0.25	0.23	0.81
r_k (kbps)	212	391	219	830	308	650	924	138
c_k	1.25	2.37	1.14	1.16	0.71	2.31	1.39	6.24
α'_k	0.03	0.04	0.06	0.05	0.02	0.03	0.02	0.04

throughput which denotes the throughput achieved with no sensing error and zero sensing time (i.e. $\sum_{k=1}^N r_k$). We observe that both the uniform and non-uniform sensing subslots cases, which refer to the MSJD and the proposed SMJD, respectively, remarkably outperform the MJD. We also observe that SMJD achieves superior performance compared to the MSJD. Two facts can be concluded. First, as opposed to the MJD strategy, the sensing time τ is a critical parameter which should be dynamically assigned due to the channel fluctuations and fading effects. This has been taken care of in the both the SMJD and MSJD. Second, other than the sensing time τ , the sensing subslot durations $\{\tau_k\}_{k=1}^N$ are greatly influential in the overall performance and should be adaptively optimized. This is adopted effectively in our framework.

In Fig. 4.4, the overall number of samples $M = \tau f_s$ is plotted versus the SNR increment above the γ_k 's listed in Table 4.1. We observe that as the channel condition improves, the optimal number of sample decreases. This illustrates the necessity for dynamically determining the sensing time as opposed to employing a fixed allocation as in MJD. Moreover, Fig. 4.4 reveals that the minimum number of samples obtained in Section 4.2.2 is not drastically smaller than the optimal number of samples. This verifies the approximation used in (4.17). We also observe that the SMJD needs a smaller sensing overhead (i.e. M) compared to the MSJD. Combining the results of Fig. 4.3 and Fig. 4.4, we conclude that the proposed SMJD framework (i.e. non-uniform sensing subslots case) achieves a greater performance compared

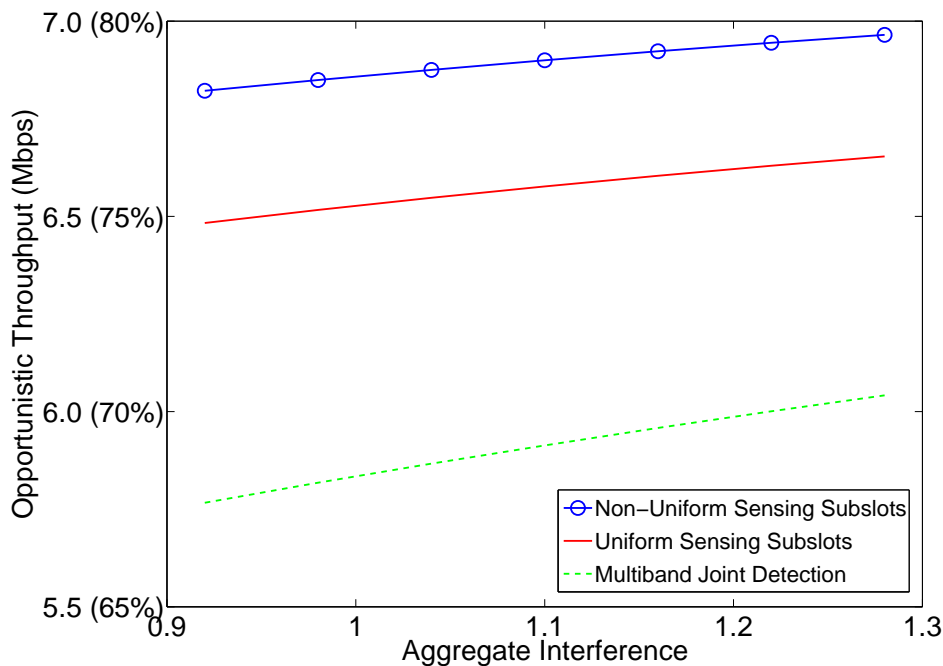


Fig. 4.3. The available opportunistic throughput for cognitive radio transmission vs. the aggregate interference to the primary network.

to the MSJD while exploiting smaller sensing overhead. Another validation to the approximation used in (4.17) is depicted in Fig. 4.5, which shows the available throughput versus the normalized minimum sensing time $\tau_{\min}^{\text{norm}}$. It can be seen that the approximation used in (4.17) becomes more precise as $\tau_{\min}^{\text{norm}}$ decreases.

4.4.2 Example 2: Decoupled Sequential Multichannel Joint Detection Framework

Here, we evaluate the proposed “decoupled sequential multichannel joint detection” (D-SMJD) framework which is given in Section 4.3.2.2. Note that the interferences on individual channels are limited separately within this framework. To make a fair comparison, two other cases are considered here. The first case, referred to as “uniform subslots D-SMJD”, solves the optimization problem (P4.6) assuming uniform sensing subslot durations which is given in Section 4.3.2.1. In the second case, referred to as “constant sensing time D-SMJD”, we assume that the sensing slot τ is a predetermined value, and consequently, the optimization problem (P4.7) is solved for $\{\tau_k\}$ as the only optimization variables set. The sensing time is assumed

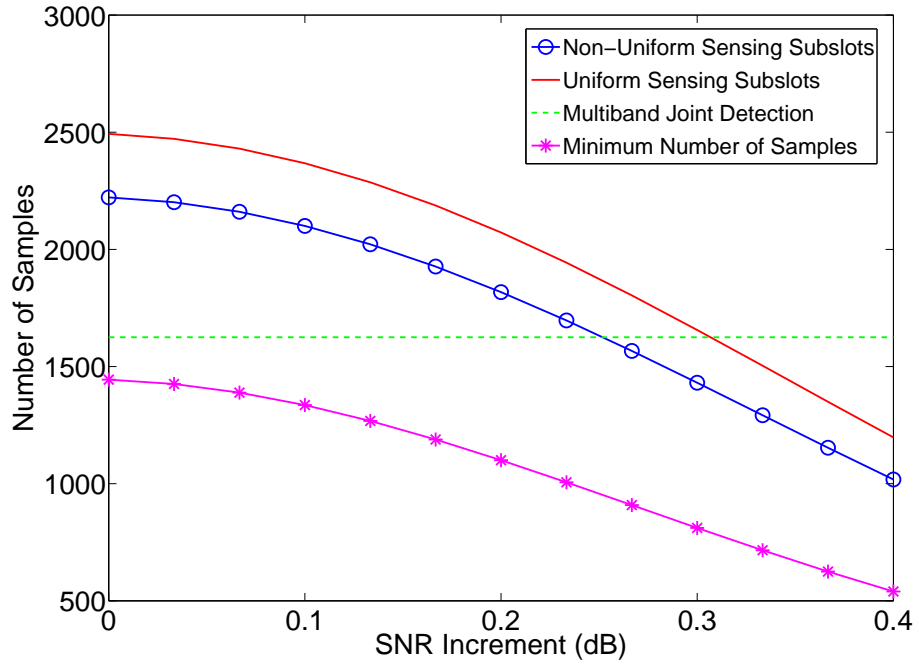


Fig. 4.4. The number of samples vs. the SNR increment (dB) above the SNRs, γ_k , listed in Table 4.1, when the aggregate interference to the primary network $\xi = 1$

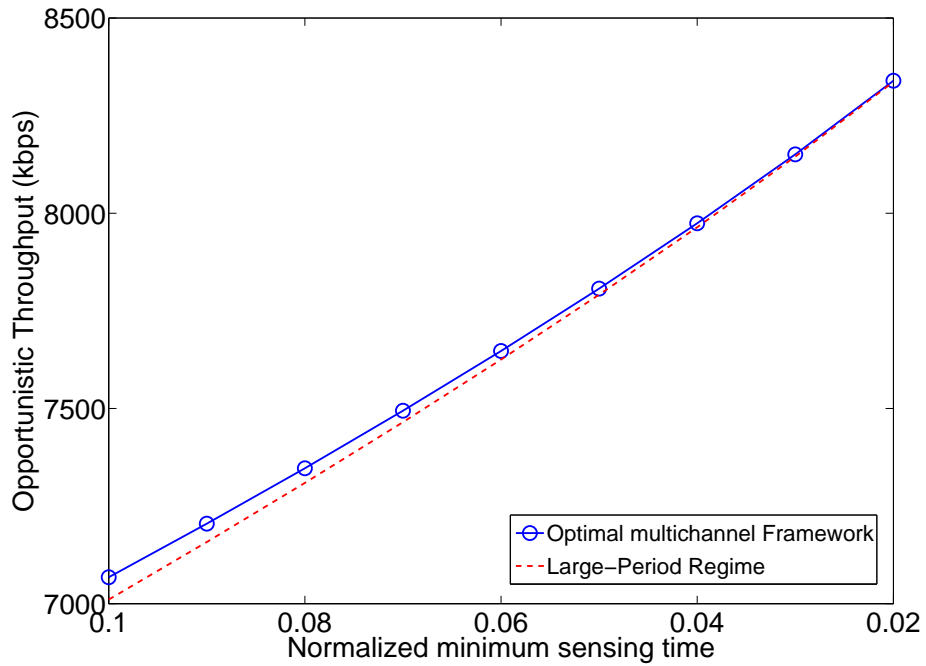


Fig. 4.5. The available opportunistic throughput for cognitive transmission vs. the normalized minimum sensing time $\tau_{\min}^{\text{norm}}$, when the aggregate interference to the primary network $\xi = 1$.

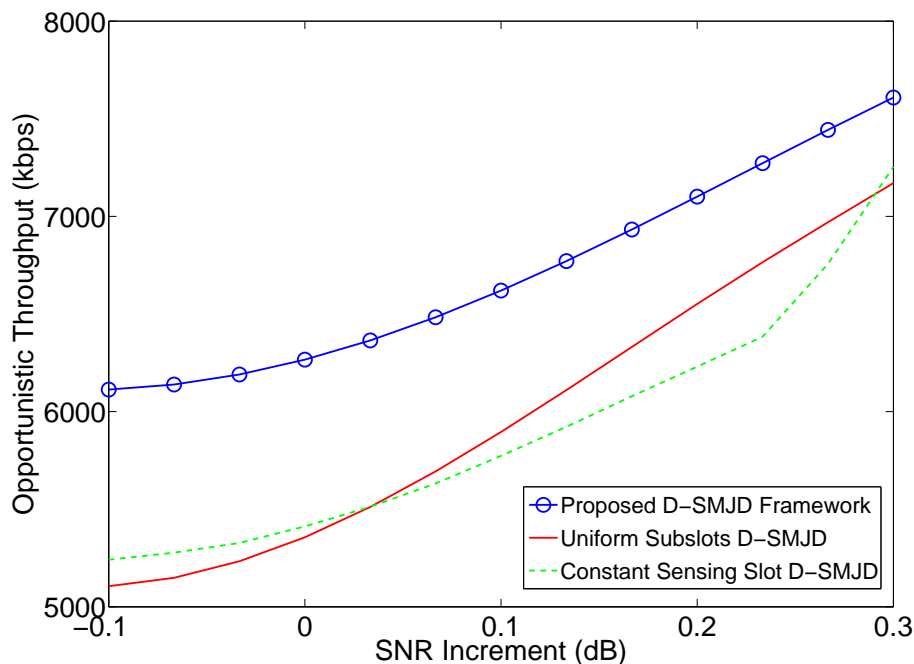


Fig. 4.6. The available opportunistic throughput vs. the SNR increment (dB) above the SNRs, γ_k , listed in Table 4.1.

to be $\tau = 40$ ms for this case. All optimization problems are convex if (4.25a) is satisfied. Fig. 4.6 plots the maximum opportunistic throughput versus the SNR increment above the γ_k 's listed in Table 4.1. It is seen that the D-SMJD framework outperforms the two other cases. In contrast to these two cases, in which either only τ or only $\{\tau_k\}$ are design parameters, D-SMJD optimizes both τ and $\{\tau_k\}$ which greatly enhances the secondary performance. As expected, when the channel conditions improve, the available throughput increases for all cases.

4.5 Summary

In this chapter, we studied the effect of non-uniform channel sensing durations for multichannel spectrum sensing and assumed that adopting different sensing durations for individual narrowband channels is viable. Consequently, considering a sequential periodic sensing scheme, we proposed two optimal multichannel spectrum sensing frameworks. Specifically, we assumed that multiple primary narrowband channels are sensed sequentially using a periodic sensing approach. We also assumed that the amount of time used for sensing different channels can be cho-

sen non-uniformly. That is, the channels-under-sense can assume different sensing time durations. Given this, we maximized the opportunistic secondary network throughput capacity, while limiting the interference imposed on the primary users. Particularly, we formulate the multichannel sensing problem as a joint optimization of the overall sensing time slot, the sensing subslots (dedicated for sensing individual channels) and individual detector parameters.

The first framework, referred to as “sequential multichannel joint detection” (SMJD) considers the aggregate interference on the primary network as the constraint function. Specifically, within the SMJD framework some relative priority coefficients, which characterize the relative costs incurred if the primary communications in the corresponding channels are interfered with, are assigned to every individual channel. That is, the overall probability of interference is aggregated (weighted) into a single functional form. In the second framework, known as “decoupled sequential multichannel joint detection” (D-SMJD), we assumed that such cost/priority coefficients used in the aggregate interference function are difficult to define for some specific applications, resulting in a tractable mathematical description of the aggregate interference being unattainable. Therefore, within the D-SMJD, we assumed that the probability of interference on each channel is limited independently, making the individual channels partially decoupled. Both formulated optimization problems, which are shown to be non-convex, are transformed into convex optimization problems under certain practical conditions.

Chapter 5

Conclusion and Future Research

Directions

5.1 Conclusion

Motivated by the need and importance of wideband/multichannel spectrum sensing in cognitive radio networks, we proposed several optimal detection frameworks for sensing over a target wideband spectrum. In Chapter 3, we proposed an optimal multiband sensing-time-adaptive joint detection (MSJD) framework for wideband spectrum sensing which collectively searches the secondary transmission opportunities over multiple frequency bands. Adopting a periodic sensing scheme as a mandatory system model and considering the amount of time used for sensing as a design parameter, we formulated the sensing problem as a *joint* optimization of the sensing slot duration and individual narrowband detectors, in which we optimized the secondary network sensing performance in an interference limited primary network. In particular, we maximized the available opportunistic throughput capacity of the secondary network while limiting the aggregate interference on the primary network. Furthermore, we demonstrated that the optimization problem is convex if certain practical constraints are applied. A special case, in which convexity holds for a wider range of conditions, was also studied.

In line with decreasing the implementation complexity of the proposed MSJD framework, we proposed a low-complexity algorithm which quickly and efficiently solves the formulated optimization problem. It was also established that the com-

plexity of the algorithm is much lower than that of other existing numerical algorithms. The results will be of particular interest when implementing a practical wideband spectrum sensing system. The complexity issue which becomes more critical when the number of individual narrowband subchannels is large will be decisive in the implementation of practical systems and is effectively taken care of in our algorithm. Generally speaking, our proposed MSJD framework adaptively and efficiently achieves a suitable tradeoff between the secondary user access and the primary network protection over a wideband frequency spectrum and can easily be implemented in practical cognitive radio systems exploiting the proposed low-complexity algorithm. Simulation results are evidence of this.

Extending the results in Chapter 3, in which the sensing slot duration is assumed to be the same in all narrowband channels, in Chapter 4, we assumed that implementing different sensing durations is feasible for multiple frequency bands. Consequently, considering a sequential periodic sensing scheme, we jointly considered the overall sensing period, individual channels' sensing subslots and each individual narrowband detector parameters as optimization variables. More specifically, we proposed two optimal multichannel detection frameworks which maximize the secondary network opportunistic throughput while limiting the overall interference on the primary network.

Within the sequential multichannel joint detection (SMJD) framework, we limited the aggregate (weighted) interference on the primary network. Pointing out that defining the so-called aggregate interference function may not be possible for some systems, we proposed decoupled sequential multichannel joint detection (DSMJD), which limits the interference on each individual channel independently (i.e. separately). We also demonstrated that the original non-convex problems can be transformed into convex optimization problems if certain practical conditions are imposed, exploiting a change of variables technique. A special case of the SMJD framework, in which convexity holds for a much wider range of conditions was also studied. The effectiveness and performance of the proposed multichannel frameworks were also confirmed through numerical simulations. In summary, this work presents multiple optimal wideband/multichannel spectrum sensing frameworks for cognitive radio networks, each suitable for specific applications.

5.2 Future Research Directions

Since it represents a fundamental study on designing optimal wideband spectrum sensing frameworks, this work can be extended (or can be considered as a basis for other studies) in several ways, a number of which are stated below.

1) The frame duration T is assumed to be fixed throughout this work. Basically, it is assumed to be chosen by the regulator and depends on the type of the primary service, end-to-end quality of service and frequency of the primary user reappearance. Optimizing the frame duration T based on the aforementioned considerations is a possible future work.

2) This study is limited to the single cognitive radio user only (i.e. the sensing task is performed by one user). Considering cooperation between multiple secondary users and designing optimal collaborative wideband sensing frameworks could be considered as an another potential research direction.

3) In this study, it is assumed that the secondary user senses all the narrowband channels simultaneously during the sensing period τ and transmits in the vacant ones in the transmission period $T - \tau$. This assumption facilitates the analysis. However, we point out that sensing one subchannel (or a number of subchannels) while transmitting in the other subchannel(s) may improve the overall sensing performance and can be integrated into the proposed frameworks.

4) In Chapter 4, we have assumed that the secondary user sequentially senses all N channels during the sensing slot τ . This may not be necessary and increases the sensing overhead, i.e. sensing a portion of N frequency bands may be enough to meet the system requirements. In line with this, one can investigate adaptively selecting the number of channels-to-sense while considering other requirements such as the secondary opportunistic throughput, the primary interference protection, etc. One possible approach can be to minimize the required number of channels-to-sense while constraining the secondary opportunistic throughput loss and the interference on the primary network.

References

- [1] Federal Communications Commission, “Spectrum policy task force report, FCC 02-155,” Nov. 2002.
- [2] Q. Zhao and B. M. Sadler, “A survey of dynamic spectrum access,” vol. 24, no. 3, pp. 79–89, May 2007.
- [3] I. Mitola, J. and J. Maguire, G. Q., “Cognitive radio: making software radios more personal,” vol. 6, no. 14, pp. 13–18, Aug. 1999.
- [4] I. F. Akyildiz, W.-Y. Lee, M. C. Vuran, and S. Mohanty, “NeXt generation/dynamic spectrum access/cognitive radio wireless networks: a survey,” *Comput. Networks (Elsevier)*, vol. 50, no. 13, pp. 2127–2159, Sep. 2006.
- [5] S. Haykin, “Cognitive radio: Brain-empowered wireless communications,” *IEEE J. Sel. Areas Commun.*, vol. 23, no. 2, pp. 201–220, Feb. 2005.
- [6] C. Cordeiro, K. Challapali, and D. Birru, “IEEE 802.22: An introduction to the first wireless standard based on cognitive radios,” *J. Commun.*, vol. 1, no. 1, pp. 38–47, Apr. 2006.
- [7] D. Cabric, S. M. Mishra, and R. Brodersen, “Implementation issues in spectrum sensing for cognitive radios,” in *Proc. 38th Asilomar Conf. on Signals, Systems and Computers*, vol. 1, Pacific Grove, CA, Nov. 2004, pp. 772–776.
- [8] H. Urkowitz, “Energy detection of unknown deterministic signals,” vol. 55, pp. 523–531, Apr. 1967.
- [9] S. M. Kay, *Fundamental of Statistical Signal Processing: Detection Theory*. New Jersey: Prentice Hall, 1998.
- [10] S. Enserink and D. Cochran, “A cyclostationary feature detector,” in *Proc. 28th Asilomar Conf. on Signals, Systems and Computers*, vol. 2, Pacific Grove, CA, Nov. 1994, pp. 806–810.

- [11] A. Sahai, N. Hoven, and R. Tandra, "Some fundamental limits on cognitive radio," in *Proc. 42nd Allerton Conf. Communication, Control, Computing*, vol. 7, no. 4, Oct. 2004, pp. 131–136.
- [12] Y. Zeng and Y.-C. Liang, "Eigenvalue-based spectrum sensing algorithms for cognitive radio," *IEEE Trans. Commun.*, vol. 57, no. 6, pp. 1784–1793, Jun. 2009.
- [13] Z. Quan, S. Cui, H. V. Poor, and A. H. Sayed, "Collaborative wideband spectrum sensing for cognitive radios," vol. 25, no. 6, pp. 60–73, Nov. 2008.
- [14] H. V. Poor, *An Introduction to Signal Detection and Estimation*. New York: Springer-Verlag, 1994.
- [15] W. Gardner, "Exploitation of spectral redundancy in cyclostationary signals," vol. 8, no. 2, pp. 14–36, Apr. 1991.
- [16] Z. Quan, S. Cui, and A. H. Sayed, "Optimal linear cooperation for spectrum sensing in cognitive radio networks," *IEEE J. Sel. Topics Signal Processing*, vol. 2, no. 1, pp. 28–40, Feb. 2008.
- [17] T. Yucek and H. Arslan, "A survey of spectrum sensing algorithms for cognitive radio applications," *IEEE Trans. Wireless Commun.*, vol. 11, no. 1, pp. 116–130, First Quarter 2009.
- [18] J. Ma, Y. Li, and B. H. Juang, "Signal processing in cognitive radio," *Proc. IEEE*, vol. 97, no. 5, pp. 805–823, May 2009.
- [19] A. Sahai and D. Cabric, "A tutorial on spectrum sensing: Fundamental limits and practical challenges," in *Proc. IEEE Int. Symposium on New Frontier in Dynamic Spectrum Access Networks (DySPAN)*, Baltimore, MD, Nov. 2005.
- [20] Y. Hur, J. Park, W. Woo, K. Lim, C. Lee, H. S. Kim, and J. Laskar, "A wideband analog multi-resolution spectrum sensing technique for cognitive radio systems," in *Proc. IEEE Int. Symp. on Circuits and Systems (ISCAS)*, Island of Kos, Greece, May 2006, pp. 4090–4093.
- [21] Z. Tian and G. B. Giannakis, "A wavelet approach to wideband spectrum sensing for cognitive radios," in *Proc. 1st Int. Conf. on Cognitive Radio Oriented Wireless Networks and Communications (CROWNCOM)*, Mykonos, Greece, June 2006.
- [22] A. Taherpour, S. Gazor, and M. Nasiri-Kenari, "Invariant wideband spectrum sensing under unknown variances," *Communications, IET*, vol. 2, no. 6, pp. 763–771, Jul. 2008.

- [23] F. Zeng, Z. Tian, and C. Li, "Distributed compressive wideband spectrum sensing in cooperative multi-hop cognitive networks," in *Proc. IEEE Int. Conf. Commun. (ICC)*, May. 2010, pp. 1–5.
- [24] Y. L. Polo, Y. Wang, A. Pandharipande, and G. Leus, "Compressive wide-band spectrum sensing," in *Proc. IEEE Int. Conf. Acoust., Speech, Signal Process. (ICASSP)*, Apr. 2009, pp. 2337–2340.
- [25] V. Havary-Nassab, S. Hassan, and S. Valaee, "Compressive detection for wide-band spectrum sensing," in *Proc. IEEE Int. Conf. Acoust., Speech, Signal Process. (ICASSP)*, Mar. 2010, pp. 3094–3097.
- [26] Z. Zhang, H. Li, D. Yang, and C. Pei, "Compressive detection for wide-band spectrum sensing," in *Proc. IEEE Int. Symposium on New Frontier in Dynamic Spectrum Access Networks (DySPAN)*, Apr. 2010.
- [27] L. Liang, Y. Liu, W. Zhang, Y. Xu, X. Gan, and X. Wang, "Joint compressive sensing in wideband cognitive networks," in *Proc. IEEE Wireless Commun. Netw. Conf. (WCNC)*, Apr. 2010.
- [28] C.-H. Hwang, G.-L. Lai, and S.-C. Chen, "Spectrum sensing in wideband OFDM cognitive radios," *IEEE Trans. Signal Process.*, vol. 58, no. 2, pp. 709–719, Feb. 2010.
- [29] G. Vazquez-Vilar, R. López-Valcarce, C. Mosquera, and N. González-Prelcic, "Wide-band spectral estimation from compressed measurements exploiting spectral a priori information in cognitive radio systems," in *Proc. IEEE Int. Conf. Acoust., Speech, Signal Process. (ICASSP)*, Mar. 2010, pp. 2958–2961.
- [30] T.-H. Yu, S. Rodriguez-Parera, D. Marković, and D. Čabrić, "Cognitive radio wide-band spectrum sensing using multitap windowing and power detection with threshold adaptation," in *Proc. IEEE Int. Conf. Commun. (ICC)*, May 2010.
- [31] M. Sanna and M. Murrioni, "Opportunistic wideband spectrum sensing for cognitive radios with genetic optimization," in *Proc. IEEE Int. Conf. Commun. (ICC)*, May 2010.
- [32] H. Li, "Reconstructing spectrum occupancies for wideband cognitive radio networks: a matrix completion via brief propagation," in *Proc. IEEE Int. Conf. Commun. (ICC)*, May 2010.
- [33] Z. Quan, S. Cui, A. H. Sayed, and H. V. Poor, "Optimal multiband joint detection for spectrum sensing in cognitive radio networks," *IEEE Trans. Signal Process.*, vol. 57, no. 3, pp. 1128–1140, Mar. 2009.

- [34] A. Ghasemi and E. S. Sousa, "Optimization of spectrum sensing for opportunistic spectrum access in cognitive radio networks," in *Proc. IEEE Consumer Commun. Netw. Conf. (CCNC)*, Las Vegas, NV, Jan. 2007, pp. 1022–1026.
- [35] Y. C. Liang, Y. Zeng, E. Peh, and A. T. Hoang, "Sensing-throughput tradeoff for cognitive radio networks," *IEEE Trans. Wireless Commun.*, vol. 7, no. 4, pp. 1326–1337, Apr. 2008.
- [36] Y. Pei, Y.-C. Liang, K. Teh, and K. Li, "How much time is needed for wideband spectrum sensing?" *IEEE Trans. Wireless Commun.*, vol. 8, no. 11, pp. 5466–5471, Nov. 2009.
- [37] R. Fan and H. Jiang, "Optimal multi-channel cooperative sensing in cognitive radio networks," *IEEE Trans. Wireless Commun.*, vol. 9, no. 3, pp. 1128–1138, Mar. 2010.
- [38] J. Ma, X. Zhou, and G. Y. Li, "Probability-based periodic spectrum sensing during secondary communication," *IEEE Trans. Commun.*, vol. 58, no. 4, pp. 1291–1301, Apr. 2010.
- [39] S. Boyd and L. Vandenberghe, *Convex Optimization*. Cambridge, UK: Cambridge University Press, 2003.
- [40] H. Cramér, *Mathematical Methods of Statistics*. Princeton University Press, 1999.
- [41] A. Papoulis and S. U. Pillai, *Probability, Random Variables and Stochastic Processes*, 4th ed. Boston, UK: McGraw-Hill, 2002.
- [42] P. Paysarvi-Hoseini and N. C. Beaulieu, "Optimal wideband spectrum sensing framework for cognitive radio systems," to appear as a full paper in *IEEE Trans. Signal Process.*
- [43] P. Paysarvi Hoseini and N. C. Beaulieu, "An optimal algorithm for wideband spectrum sensing in cognitive radio systems," in *Proc. IEEE Int. Conf. Commun. (ICC)*, Cape Town, South Africa, May 2010.
- [44] A. Goldsmith, *Wireless Communications*. Cambridge, UK: Cambridge University Press, 2006.
- [45] Initial Evaluation of the Performance of Prototype TV-Band White Space Devices, FCC/OET 07-TR-1006, Jul. 2007.
- [46] P. Paysarvi-Hoseini and N. C. Beaulieu, "On the benefits of multichannel/wideband spectrum sensing with non-uniform channel sensing durations for cognitive radio networks," submitted to *IEEE Trans. Commun.*, Sep. 2010.

- [47] P. Paysarvi-Hoseini and N. C. Beaulieu, "Sequential multichannel joint detection framework with non-uniform channel sensing durations for cognitive radio networks," submitted to *IEEE Int. Conf. Commun. (ICC)*, Kyoto, Japan, Jun. 5-9, 2011.
- [48] P. Paysarvi-Hoseini and N. C. Beaulieu, "Improved multichannel spectrum sensing in cognitive radio systems," submitted to *IEEE Int. Conf. Acoust., Speech, Sig. Process. (ICASSP)*, Prague, Czech Republic, May 22-27, 2011.